THE PERFORMANCE OF A CURVILINEAR VERSUS A RECTANGULAR BASEMENT FOUNDATION DESIGN IN EXPANSIVE CLAY SOILS

by

Michael James Gardiner

B.A., The Colorado College, 1985

B.S., University of Colorado, Denver, 2001

A thesis submitted to the

Faculty of the Graduate School of the

University of Colorado in partial fulfillment

of the requirements for the degree of

Master of Science

Civil Engineering

2013

This thesis for the Master of Science degree by

Michael James Gardiner

has been approved for the

Civil Engineering Program

by

Nien-Yin Chang, Chair

Brian T. Brady

Yail Jimmy Kim

April 10, 2013

Gardiner, Michael James (Master of Science, Civil Engineering)

The Performance of a Curvilinear Versus a Rectangular Basement Foundation Design in Expansive Clay Soils

Thesis directed by Professor Nien-Yin Chang

ABSTRACT

Shallow foundation design in expansive soils has generally been approached in the industry using a typical pier/beam or spread footing/foundation wall and reinforcement design. The addition of supporting piers anchored in stable soils and excavated expansion areas under beam elements have modified a traditional foundation design for expansive soils. This traditional approach to foundation design uses designs that mitigate around the swelling effects, rather than designing to take advantage of, or resist the imposed forces.

This research defines a new shallow foundation design that uses a curvilinear structure to take advantage of the forces exerted on the foundation by the expansive forces of the soil. In addition, the design allows for a cast-in-place or precast implementation. The curvilinear foundation design was modeled using LS DYNA Finite Element analysis and compared to a traditional rectangular foundation design using 3D models. In addition, the soil and concrete models were evaluated by comparing the LS DYNA model results (deflection, shear, tensile/compression) for both foundation designs.

Also included in the research is the analysis of a discontinuity (window) in the structural design and the effects of the discontinuity on the structure.

The form and content of this abstract are approved. I recommend its publication.

Approved: Nien-Yin Chang

DEDICATION

I dedicate this thesis to my wife Jerre and express my gratitude and appreciation for her support, encouragement and sacrifice throughout the extent of my studies. She has been the foundation on which I have built my life and I am truly blessed to have such a wonderful partner. I would also like to dedicate this thesis to my father and mother, John and Viola Gardiner, for instilling in me perseverance to complete what I have started and for their support. I would also like to include a special dedication to Jean Durham for her continuous encouragement throughout the many years of research and study.

ACKNOWLEDGEMENT

I would like to express my sincere appreciation and heartfelt thanks to my advisor Professor Nien-Yin Chang for his continuous guidance, support and unwavering encouragement throughout my studies and the completion of this research. The catalyst for this research began with Dr. Chang during coursework in Intermediate Foundation Engineering in the fall of 2001. Dr. Chang's inexhaustible patience and personal commitment allowed me the freedom and time to manage multiple priorities during this course of study. In the end I have the privilege of calling Dr. Chang my friend.

I would like to express my gratitude to Dr. Brian Brady and Dr. Jimmy Kim for serving on my defense committee and providing me with their valuable inputs and comments to improve the content of this thesis.

TABLE OF CONTENTS

LIST OF TABLES

Table

LIST OF FIGURES

Figure

1. Introduction

Expansive (swelling) soils are extremely common in the Front Range area of Colorado and can be found on almost every continent across the globe. The destructive effects caused by expansive soils have been reported in numerous countries such as the United States, Canada, Australia, China, Israel, South Africa and India (Nelson and Miller, 1992; Steinberg, 1998). It has been widely reported that losses due to expansive soils have been measured in several billions of dollars yearly (Nelson and Miller, 1992). The cost of repairing damage caused by swelling soils amounts to more than the cost for all other natural hazards combined. This is especially true of light structures, pavements and service piping.

Expansive soils are capable of mobilizing huge vertical and lateral pressures which, in turn, become a hazard primarily to structures and pavements built on top of the expansive soil or within the volume of expansive soils that are subject to moisture changes. The damage may not manifest itself immediately, depending on the soil composition, moisture history, future moisture/desiccation cycling and type of foundation construction. Up until now, mitigation in the industry has followed two primary paths: mitigation of existing structures by adjusting drainage and/or underpinning; and mitigation of the design by using pier and beam foundations with drainage implemented at the foundation to prevent soil expansion. To a lesser extent, changing the soil properties by chemical mixing, removal of the offending soils or mixture of the soils with more suitable soil has been implemented in the industry.

Although the current industry standards for mitigation of light structures constructed in expansive soils, as described above, offer piece of mind against catastrophic damage, long term stability is not guaranteed. Over time, severe drought and flooding cycles can directly influence the foundation performance and exceed the design mitigations implemented. In addition, changes in soil chemistry can occur during periods of high moisture exposure negating the benefits of soil treatment methodologies. Over time, changes in soil drying can occur due to rises in the ambient temperatures and/or the growth of vegetation within the soil mass. With unprecedented weather events taking place all over the globe, the design of structures must rely less on mitigation of moisture intrusion and more on foundation designs that take advantage of the potential forces mobilized by the soil.

1.1 Purpose of the Study

The purpose of this study is to introduce a foundation design that accounts for and reacts to the pressures generated by expansive soils. It allows for changes in the moisture content of the expansive soil and is designed to accommodate the resulting forces. This approach is consistent with the intent of the International Building Code and the American Concrete Institute's 318-05: Building Code Requirements for Structural Concrete.

1.2 Scope of Study

The primary scope of this study is to examine the current design and construction practices for light foundation designs relative to expansive clay soil pressures with changing soil properties. Included in the study is a curvilinear

foundation design approach/solution that works with the in situ soil conditions to resist the changing lateral pressures and soil heave. The study includes a Finite Element Model and analysis of a new foundation design compared to a traditional rectangular foundation design used in industry today.

1.3 Organizational Outline

A brief description of each chapter in this study is presented below.

- Chapter 1 introduces the issue of expansive soils as they relate to foundation design and damage.
- Chapter 2 presents a review of clay soil properties and experimental techniques used in determining swell potential and lateral swell pressure. The risk of foundation movement relates to the amount of vertical and horizontal heave/swell that will occur. Heave depends on more than just the percent swell of the soil. Calculations of predicted heave must also take into account the stress or surcharge applied to the soil when the soil is inundated with water. Various methods are widely used in the industry to classify swell potential and determine soil properties related to unsaturated clays. One method commonly used to determine the expansion potential of a soil is based on the index properties (Holtz and Gibbs 1956; Holtz and Kovacs 1981). This requires knowledge of the clay content and the plasticity index. These properties can be determined by performing a gradation test including the Atterburg limits. Another method widely used for estimating the expansion potential of a clay soil uses soil classification

information. Seed et al. (1962) developed a classification chart method (activity) based on the amount and type of clay particles in the soil. In addition, experimental methods are also used to determine swell induced strains, swell potential and swell pressure. These are typically accomplished by means of a consolidation-swell type test such as ASTM D4546, One-Dimensional Swell or Collapse of Cohesive Soils.

- Chapter 3 addresses the application of lateral pressures resulting from the soil mass, surcharge and the water table. It also describes the methods that are used to define the lateral pressure profile on a structure.
- Chapter 4 reviews the current design practices that are used for foundation wall design as described in the International Building Code (International Code Council, 2005), the International Residential Code for One- and Two-Family Dwellings (International Code Council, 2005), and the American Concrete Institute, 318-05: Building Code Requirements for Structural Concrete.
- Chapter 5 presents a new, curvilinear foundation design approach to effectively use the properties of an expansive soil to achieve long-term survivability and serviceability of the structure. This includes, as an assumption, changing soil conditions that prove to be problematic to traditionally designed foundations including moisture and climatic changes, soil chemistry changes and changes in drainage.

- Chapter 6 presents the Finite Element Analysis approach for the new foundation design using LS-DYNA software (Livermore Software Technology Corporation). The analysis parameters for structural properties of the foundation and loading due to the soil are presented. Also discussed is a traditional rectangular foundation design for comparison.
- Chapter 7 presents the findings of the analysis. It compares the new curvilinear foundation design to the traditional rectangular design, evaluating wall stress versus applied loading.
- Chapter 8 presents the discussion of the results and a comparison of performance between the traditional rectangular foundation design and the curvilinear design.
- Chapter 9 presents the summary and conclusions of the research/analysis and recommendations for future, related research.

2. Properties of Cohesive Soils

2.1 Introduction - Expansive Soils

Clay soils are often described as cohesive, fine-grained soils having plasticity and containing clay minerals such as kaolinite, halloysite, montmorillonite, illite, chlorite and vermiculite (Holtz & Kovacs, 1981). However, not all fine-grained soils are cohesive and/or clay. Silts, for example, are classified as fine-grained and granular but are not cohesive and are not plastic. For clay soils, grain size distribution has little influence on the properties of the clay whereas for granular soils the grain size distribution and the grain shape can have marked effects on the properties of the soil. Additionally, water content is relatively unimportant (with a few exceptions) for granular soils but has a definite influence on clay soils. Silts are fine-grained and granular but are not plastic and are non-cohesive. Their strengths, like sands, are essentially independent of water content.

Clay minerals owe their unique properties and behavior to some very distinct characteristics. Clay minerals are extremely small particles (< 1 μm diameter) that are electrochemically active. They are affected by the quantity and type of clay minerals present, the moisture content, the type and chemistry of the soil water surrounding the clay particles, the arrangement, soil density and specific surface area of the clay particles. In a mixed clay and soil mass, as the clay content increases, the behavior of the soil mass is increasingly governed by the clay fraction properties. As the clay content approaches and exceeds approximately 50%, the sand and silt grains in the mixed clay/soil mass are

“floating” within the clay matrix which dominates the soil mass behavior (Holtz & Kovacs, 1981).

2.2 Soil Classification

The purpose of soil classification is to provide for a common means of determining or predicting the behavior of soils and/or evaluating soils for engineering purposes. There are numerous soil classification systems in use. In the United States, the Unified Soil Classification System (USCS) is the most widely used soil classification system for structural considerations (Howard, 1977) while the American Association of State Highway and Transportation Officials (AASHTO) classification system is typically used for pavement design. The Unified Soil Classification System (USCS) was initially developed by Casagrande in1948 and later modified by Casagrande in 1952.

Within the USCS (Figure 2.1), soil materials are classified into three main groups: Coarse-grained, Fine-grained and Peat (highly organic soils) depending on the predominant particle sizes and make-up within the soil matrix. Soils are identified within the three major groups primarily on the basis of particle sizes and changes to the soil properties and volume when interacting with water. Coarse-grained soils (sands and gravels) contain particles that are visible to the naked eye (larger than about 0.003 in. [0.075 mm]) and are generally described as cohesionless, with engineering behavior primarily influenced by the composition of particle sizes, particle shape, and relative density. Coarse-grained soils are further defined within the USCS as greater than 50% (by dry mass) retained on the number 200 Standard Sieve with a mesh opening of 0.075mm.

Subdivisions within this classification system are largely based on particle size: gravels (75mm to 4.75mm) and sands (4.75mm to 0.075mm). Both sands and gravels are further subdivided into four secondary groups (GW, GP, GM, GC; SW, SP, SM, SC). The four secondary classifications are based on whether the soils are well graded, poorly graded, contain silt-size particles or contain clay-size particles.

Fine-grained soils include silts and clays containing particles that are not visible to the naked eye. Fine-grained soils are those composed primarily of silt and clay-sized particles smaller than 0.075 mm. Fine-grained soils are defined as having 50 percent or more (by dry mass) of soil particles passing through the number 200 Standard Sieve. Silts and clays are largely distinguished based on the plasticity properties of the soil, as measured by the soils' Atterberg Limits. Both silts and clays are further subdivided into three secondary groups (ML, CL, OL; MH, CH, OH). The three secondary classifications are based on the inorganic and organic nature of the soil and on its plasticity. Silts may be either cohesive or cohesionless and are granular materials with sizes falling between sands and clays. Silts may occur as a soil or as suspended sediment. Clays, on the other hand, are cohesive soils, with engineering behavior primarily influenced by plasticity and cohesion. Soils containing high natural organic content comprise the third major group. Peats (organic soils) can be of extremely low strength and high compressibility, depending on organic content and composition, and geologic history.

Unified Soil Classification System (USCS)					
Coarse-grained soils (More than 50% retained on No. 200 (0.075mm) sieve)	Gravels (More than 50% of coarse fraction retained on no. 4 (4.75 mm) sieve)	GW	Well-graded gravels or gravel-sand mixtures, little or no fines	Less than 5% fines[*]	Cu ≥ 4 and 1 ≤ Cc ≤ 3
		GP	Poorly graded gravels or gravelly sands, little or no fines	Less than 5% fines[*]	Does not meet Cu and/or Cc criteria listed above
		GM	Silty gravels, gravelsand-silt mixtures	More than 12% fines[*]	Minus no. 40 soil plots below the A line
		GC	Clayey gravels, gravelsand-clay mixtures	More than 12% fines[*]	Minus no. 40 soil plots on or above the A line
	Sands (50% or more of coarse fraction passes no. 4 (4.75 mm) sieve)	SW	Well-graded sands or gravelly sands, little or no fines	Less than 5% fines[*]	Cu ≥ 6 and 1 ≤ Cc ≤ 3
		SP	Poorly graded sands or gravelly sands, little or no fines	Less than 5% fines[*]	Does not meet Cu and/or Cc criteria listed above
		SM	Silty sands, sand-silt mixtures	More than 12% fines[*]	Minus no. 40 soil plots below the A Line
		SC	Clayey sands, sandclay mixtures	More than 12% fines[*]	Minus no. 40 soil plots on or above A line
Fine-grained soils (50% or more passes no. 200 (0.075mm) sieve)	Silts and clays (Liquid limit less than 50)	ML	Inorganic silts, rock flour, silts of low plasticity	Inorganic soil	PI < 4 or plots below A line
		CL	Inorganic clays of low plasticity, gravelly clays, sandy clays, etc.	Inorganic soil	PI > 7 and plots on or above A line [†]
		OL	Organic silts and organic clays of low plasticity	Organic soil	LL (ovendried)/ LL (not dried) < 0.75
	Silts and clays (Liquid limit 50 or more)	MH	Inorganic silts, micaceous silts, silts of high plasticity	Inorganic soil	Plots below A line
		CH	Inorganic highly plastic clays, fat clays, silty clays, etc.	Inorganic soil	Plots on or above A line
		OH	Organic silts and organic clays of high plasticity	Organic soil	LL (oven dried) / LL (not dried) < 0.75
Peat	Highly Organic	PT	Peat and other highly organic soils	Primarily organic matter, dark in color, and organic odor	

[*]Fines are those soil particles that pass the no. 200 sieve. For gravels with 5 to 12 percent fines, use of dual symbols required (i.e., GW-GM, GW-GC, GP-GM, or GP-GC). For sands with 5 to 12 percent fines, use of dual symbols required (i.e., SW-SM, SW-SC, SP-SM, or SP-SC).

[†]If 4 ≤ PI ≤ 7 and plots above A line, then dual symbol (i.e., CL-ML) is required.

Figure 2.1: Grain-size Classification System (after U.S. Army Waterways Experiment Station (1960) and Howard (1977))

2.2.1 Gradation of Soils

Gradation tests are performed on a soil to determine the particle size distribution which is used in the classification of a soil. The gradation of a soil has a major effect on its mechanical and hydraulic properties and enables an evaluation of engineering characteristics such as permeability, strength, swelling potential, and susceptibility to frost action. The tests consist of two types: sieve analysis for coarse-grained soils (sands, gravels) and hydrometer analysis for fine-grained soils (silts, clays). Materials containing both types of soils

(sands/gravels and silts/clays) are tested by both methods and the results are merged to create one particle size distribution result.

Gradation of coarse-grained soils consists of a mechanical grain size analysis. The analysis consists of taking an oven-dried soil sample and subjecting it to a series of standard sieves with progressively smaller openings while mechanically shaking the sieves. Once complete, the amount of material retained on each of the sieves is weighed. The total percentage passing each sieve is determined and the data plotted on a semilogarithmic graph of grain size versus percent finer by weight (Figure 2.2). Based on the results of the particle size distribution testing, soils can be classified as poorly-graded (uniform), when it contains a narrow distribution of particle sizes or well-graded, when the soil has a wide range of particle sizes. The flatter the grain size curve the larger the range of particle sizes found in the soil and the steeper the curve the fewer the particle sizes. Generally speaking, a well-graded soil has a curve that is smooth and contains particles over a relatively large range of sizes while a poorly-graded soil has a curve where a high portion of the soil particles contain sizes within a narrow band. If particles of large and small sizes are present with a low proportion of particles in the intermediate sizes the soil is categorized as a gap-graded soil (McCarthy, 1998).

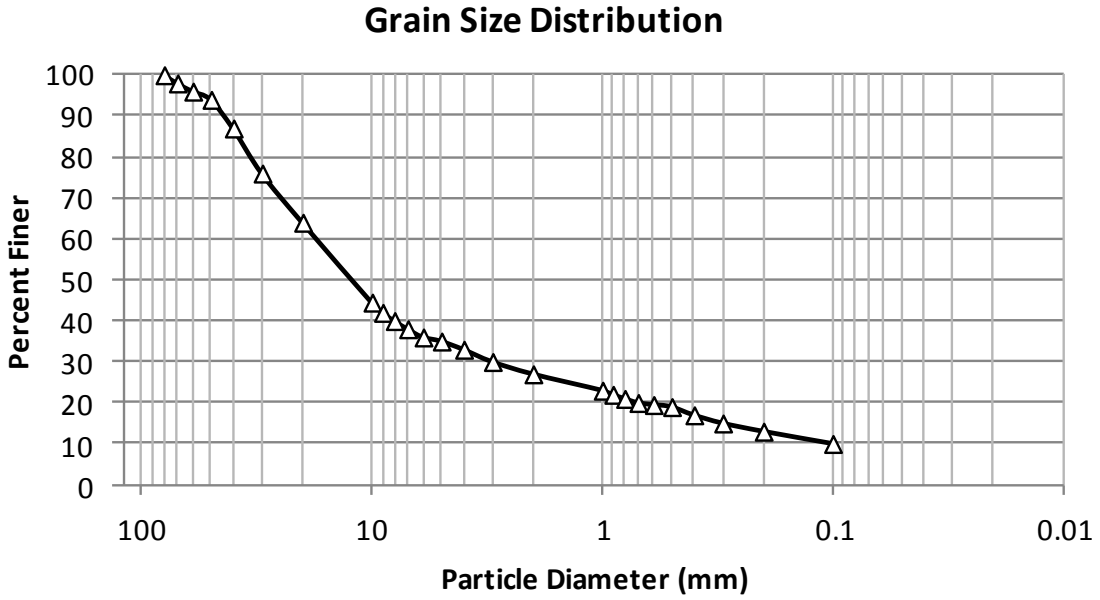

Figure 2.2: Grain Size Distribution (after ASTM International, D2487-11)

A hydrometer analysis is performed on soils finer than the No. 200 sieve (0.075 mm) since a sieve analysis is impractical for small diameter particles (grains). The hydrometer analysis is a sedimentation process where the rate of settlement of a soil in water is measured as an indication of particle size. The test is based on Stoke's law for falling spheres in a viscous fluid where the terminal velocity of fall depends on the grain diameter and the densities of the grains in suspension and of the fluid. The particle diameter can be determined from knowledge of the distance of fall and the time. Stokes law does not apply to particle sizes below 0.0002 mm as these particle sizes are influenced by Brownian movement (U.S. Army Corps of Egineers, 1998).

Interpretation of the gradation analysis focuses on the range of particle diameters found in the sample. This information can be readily determined from

the semi-logarithmic grain size distribution curve (Figure 2.2). The particle size representing a given "percentage smaller" can be directly determined from reading the particle size from the specific "percentage finer" number. Sizes commonly used in calculating uniformity coefficients are the percentage smaller than 10%, 30% and 60% and are denoted D_{10}, D_{30} and D_{60}, respectively. As a measure of the gradation of a soil, the coefficient of uniformity (C_u) is used to describe a soil's range of particle sizes. It is defined as the ratio of the D_{60} size of the soil (the particle size in mm where 60% of the soil particles are finer than) to the D_{10} size (the particle size in mm where 10% of the soil particles are finer than). The uniformity coefficient (C_u) is calculated as the following ratio:

$$C_u = \frac{D60}{D10} \qquad 2.1$$

Where: D60 = soil particle diameter at which 60% of the mass of a soil sample is finer and D10 = the diameter at which 10% of the mass of a soil sample is finer.

The D_{10} is often referred to as the effective particle size and is utilized in many empirical methods to characterize the soil as a whole, particularly with regard to hydraulic conductivity. Generally, the higher the value of the coefficient of uniformity (C_u) the greater the range of particle sizes in the soil sample.

Another quantity that may be used to judge the gradation of a soil is the coefficient of curvature, designated by the symbol C_c. The coefficient of curvature is defined as the following:

$$C_c = \frac{D30^2}{D60xD10} \qquad 2.2$$

Where: D60 = soil particle diameter at which 60% of the mass of a soil sample is finer, D10 = soil particle diameter at which 10% is finer and D30 = soil particle diameter at which 30% of the mass of the soil is finer.

A well-graded soil is defined as having a good representation of all particle sizes from the largest to the smallest and the shape of the grain size distribution curve is considered "smooth." In the USCS, well-graded gravels must have a C_u value > 4, and well-graded sands must have a C_u value > 6. For well-graded sands and gravels, a C_c value from 1 to 3 is required. Sands and gravels not meeting these conditions are considered poorly graded.

2.2.2 Atterberg Limits

Atterberg limits are limits of moisture content (mass of water in the soil to the mass of the solid particles) used to define fine-grained soil behavior. In engineering practice, three of the limits (the liquid, plastic and shrinkage limits) are commonly used.

The Liquid Limit (LL) is the water content, in percent, that defines where the soil changes from a viscous, fluid state to a plastic state. Above this point the soil behaves as a liquid, while below this point the soil behaves as a plastic material. The Liquid Limit can be measured using the (Casagrande) liquid limit device.

The Plastic Limit (PL) is defined as the water content, in percent, where the soil changes from a plastic state to a semi-solid state. Above this point the soil behaves as a plastic material, while below this point the soil behaves as a semi-solid. The Plastic Limit is also the moisture content at which a soil crumbles when rolled into a thread of 1/8 inch in diameter (Das, 2002).

The Shrinkage Limit (SL) is defined as the moisture content where the soil volume will not reduce further if the moisture content is reduced. Above this point the soil behaves as a semi-solid, while below this point the soil behaves as a solid.

Plasticity Index (PI) is defined as the difference between the moisture content at the Liquid and Plastic Limits. This represents the range of water content where a material behaves plastically (Das, 2002).

$$\boldsymbol{PI = LL - PL} \qquad 2.3$$

Since the PI is determined from Atterberg Limits testing on the fraction of soil that passes the no. 40 sieve (0.425 mm), a correction factor is applied for soils that contain a large fraction of particles coarser than the no. 40 sieve.

Fine-grained (cohesive) soils can be classified either as low or high compressibility materials based on the results of the Atterberg Limits tests. By plotting the Plasticity Index versus the Liquid Limit the classification can be determined graphically (Figure 2.3).

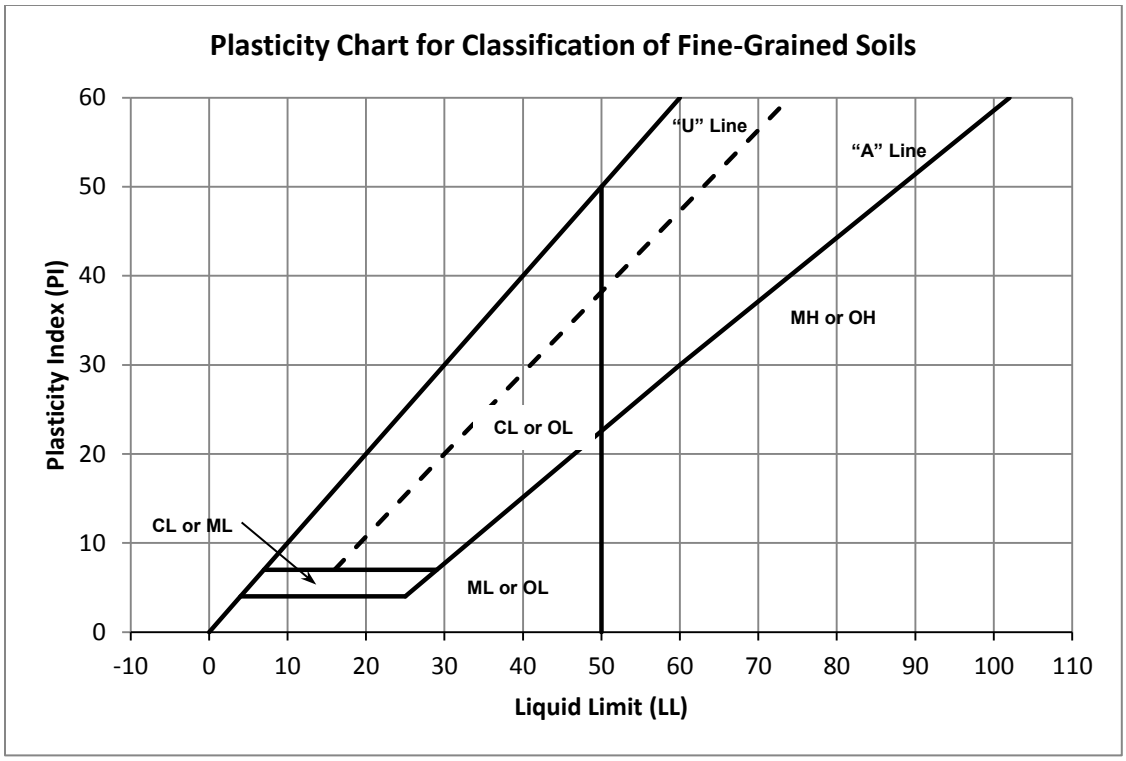

Figure 2.3: Plasticity Index versus Liquid Limit (ASTM D2487 – 11, Standard Practice for Classification of Soils for Engineering Purposes)

The A-Line separates clay classifications and silt classifications, while the U-Line represents an approximate upper limit of LL and PI combinations for natural soils.

2.2.3 Activity

A variety of soil engineering properties have been correlated to the liquid and plastic limits as well as being used to classify fine-grained soils according to the Unified Soil Classification System. Knowledge of the Atterberg limits for a cohesive soil and the natural moisture content can tell a good deal about its geologic history and engineering performance (Figure 2.4).

Probable Expansion as Estimated from Classification Test Data				
Degree of Expansion	**Probable Expansion as a % of the Total Volume Change (Dry to Saturated Condition)***	**Colloidal Content (% - 1um)**	**Plasticity Index, PI**	**Shrinkage Limit, SL**
Very High	>30	>28	>35	<11
High	20 - 30	20 - 30	25 - 41	7 - 12
Medium	10 -20	13 - 23	15 - 28	10 - 16
Low	<10	<15	<18	>15

Figure 2.4: Probable Clay Expansion as Estimated from Classification Test Data (after Holtz, 1959)

The presence of small amounts of certain types of clay minerals can have significant impacts on the soil's properties. The identification of the type and amount of the clay minerals present can help in determining or predicting the soil's behavior or to determine how to minimize the effects of the clay minerals present (McCarthy, 1998). Indirect methods are available to determine information about the type and effects of clay minerals in a soil that are relatively easy to perform and give qualitative, if not quantitative, results (Figure 2.5).

Characteristics of Common Clay Minerals								
					Atterberg Limits			
Mineral Group	**Basal Spacing (Å)**	**Particle Features**	**Interlayer Bonding**	**Specific Surface (m^2/g)**	**Liquid Limit % (LL)**	**Plastic Limit % (PL)**	**Shrinkage Limit % (SL)**	**Activity Ratio (PI / % clay)**
Montmorillonite	9.6	Thin, filmy, flakes > 10A X 1.0 to 10 µm	Very weak van der Waals bonds	700 - 840	100 - 900	50 - 100	8.5 - 15	7.2
Illites (Mica-like)	10	Thin, stacked plates 0.003 to 0.1 X 1.0 to 10 µm	Strong potassium bonds	65 - 100	60 - 120	35 - 60	15 - 17	0.9
Kaolinites	14.4	Thick, stiff 6-sided flakes 0.1 to 4 X 0.05 to 2 µm	Strong hydrogen bonds	10 - 20	30 - 100	25 - 40	25 - 29	0.38

Figure 2.5: Characteristics of Common Clay Minerals (after Mitchell, 1976)

One such method is the clay Activity and is determined from a relationship of the plasticity of the clay and the quantity of clay-sized particles. For a given amount of clay mineral the plasticity resulting in a soil varies for different clay minerals. The Activity, defined as

$$\boldsymbol{A} = \frac{\boldsymbol{Plasticity\ Index}}{\%\ \boldsymbol{by\ Weight\ Finer\ than\ 2\mu m}} \qquad 2.4$$

Where the percent by weight finer than 2 μm is equal to that portion of the soil (by weight) consisting of particles <0.002 mm. This information can be determined by the hydrometer analysis (ASTM International D422-63).

Three classes of clays according to activity suggested by Skempton (1953) are inactive (A < 0.75), normal (0.75 ≤ A ≤ 1.25) and active (A > 1.25). The clays with the highest activity have the most potential for expansion.

Table 2.1: Clay Activity (after McCarthy, 1998)

Activity	Classification
<0.75	Inactive Clay
0.75 – 1.25	Normal Clay
>1.25	Active Clay

Typical values of activities for various clay minerals range from quartz (activity = 0) to sodium montmorillonite (activity = 4 to 7) at the extremes while

Illite (activity = 0.9) and calcium montmorillonite (activity = 1.5) fall somewhere in between.

2.3 Clay Minerals

The cohesive properties of natural soils are related to the presence of clay minerals (e.g., kaolinite, halloysite, montmorillonite, illite, chlorite and vermiculite). The most important of these clay minerals associated with expansion are kaolinite, montmorillonite and illite. All are very small crystalline substances of hydrous aluminosilicates (phyllosilicates or layered silicates). The crystalline substances are a result of weathering (physical or chemical) of parent rock materials, primarily igneous and sedimentary rocks (G.W. Donaldson, 1969).

Three of the most important clay mineral groups are the kaolinites (generally non-expansive), the mica mineral group which includes the illites and vermiculites (can be expansive), and the smectites which includes montmorillonite (can be highly expansive). The swelling potential varies widely with the type of clay mineral and is generally ranked in the following order from most to least expansive: montmorillonite, illite, kaolinite (Lambe and Whitman, 1969).

Clay minerals are generally constructed of stacks of two types of sheets: silica tetrahedral sheets and alumina octahedral sheets. Each sheet is only angstroms thick ($1.0000e^{-10}$ m) and can be thousands of angstroms wide in each of their lateral dimensions. The individual crystals can only be observed with an electron microscope and their structure has been observed using x-ray

diffraction. Each family of clay mineral type consists of vertical stacks of these elementary plates or sheets in differing arrangements. Each plate or sheet has a repeating atomic structure consisting of the two primary crystal sheets.
The silica tetrahedral sheets are constructed of individual tetrahedron molecules with the general composition of SiO_4 (in some instances contain substitutions of aluminum ions for silica ions). The alumina octahedral sheets are constructed of individual octahedron molecules with the general composition of $Al(OH)_6$ (Gibbsite) with substitutions of either iron or magnesium (Brucite) for aluminum ions. If all of the anions are hydroxyls and at least 2/3 of the cation positions are filled with aluminum the mineral is labeled gibbsite. If the cation positions are filled with magnesium instead of the aluminum then the mineral is labeled brucite. The arrangement of the stacking of these sheets, with the various metal ion substitutions throughout the crystal lattice, makes up the different clay mineral types (Holtz and Kovacs, 1981).

The basic tetrahedral sheet is a combination of silica tetrahedral molecules. The tetrahedral molecule consists of four oxygen atoms at each of the corners of the tetrahedron with a silicon atom at its center (tetrahedral sheet Figure 2.6). The oxygen atoms at the base of a single tetrahedron molecule are combined to form continuous sheets with the base oxygen atoms arranged in a single plane.

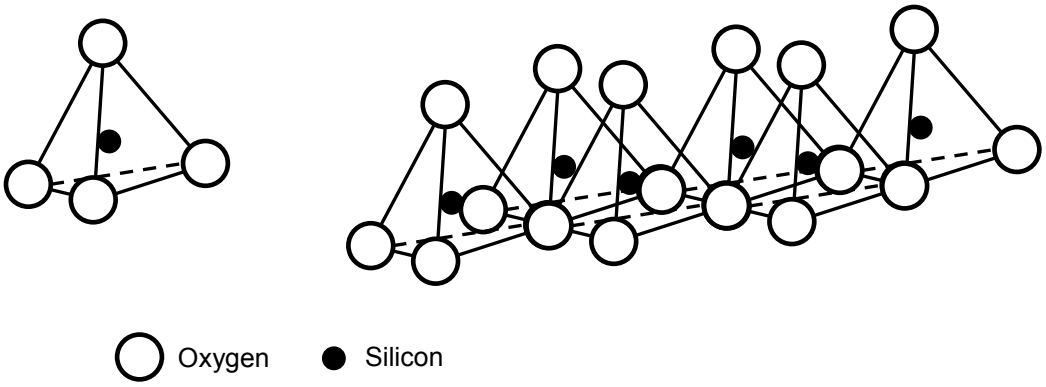

Figure 2.6: Silica Tetrahedron and Silica Tetrahedral Molecules (after Grim, 1968)

The basic octahedral sheet is a combination of octahedral molecules. The octahedral molecule consists of six oxygen atoms or hydroxyl molecules (Oxygen-Hydrogen molecule) with aluminum, magnesium, iron, or other atom at its center (single octahedral molecule Figure 2.7). The oxygen atoms or the hydroxyl molecules are positioned such that two planes are formed within the sheet. Substitutions of the cations within the octahedral sheet are common and produce different clay minerals.

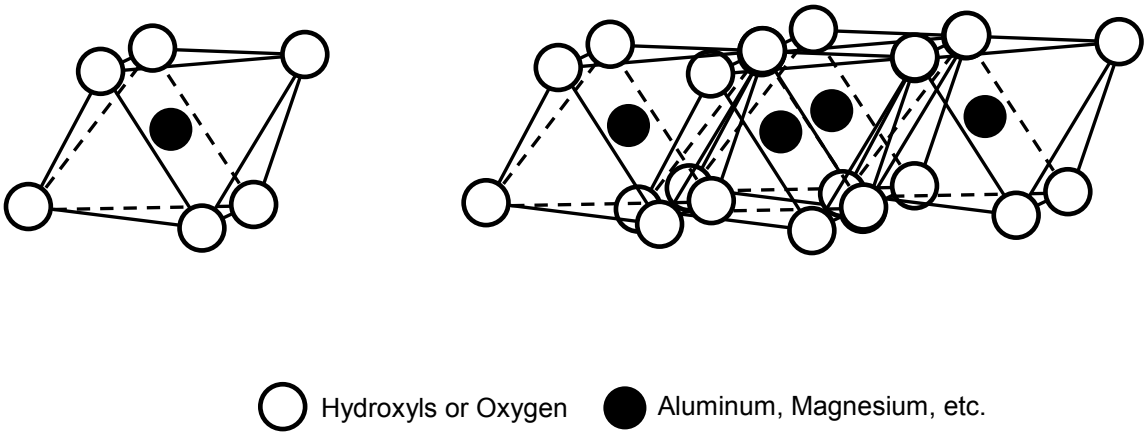

Figure 2.7: Alumina Octahedron and Alumina Octahedral Molecules (after Grim, 1968)

All clay minerals contain the two basic tetrahedral and octahedral sheets and are stacked together in various combinations with differing substitutions of cations within the molecules to form the minerals. The various types of clay minerals result from the stacking of the specific tetrahedral and octahedral sheets and the type of chemical bonding between each sheet. The variety of mechanical and physical properties of different clays is a result of the unbalanced electrical charges that are a result of certain cationic substitutions and the overall net electronegative polarity resulting from the sheet stacking arrangements. This includes differences in cohesion, water absorption and expansion found in the different clay minerals.

The more common clay minerals found in clay soils within the Unites States are described in the following sections.

2.3.1 Kaolinite

Kaolinite minerals are formed of repeating layers of one tetrahedral (silica) sheet and one octahedral (alumina or gibbsite) sheet and are classified as 1:1 minerals. The two layers are held together by hydrogen bonding (Hydroxyl ions on the octahedral sheet to oxygen atoms on the tetrahedral sheet) forming a single layer (Figure 2.8). The strong hydrogen bonding resists swelling stresses when water is present and also allows the construction of large crystal structures. These mineral layers are approximately 0.72 nm (7.2 A) in thickness and extend laterally in both directions indefinitely. Kaolinite crystals are constructed of repeating layers of the 0.72 nm mineral layer. It is not uncommon to have kaolinite crystals 70 to 100 layers thick (Holtz and Kovacs, 1981). The cation exchange capacity of Kaolinite is very low (3 to 15 meq/100 gm) owing to little substitution within the mineral sheets.

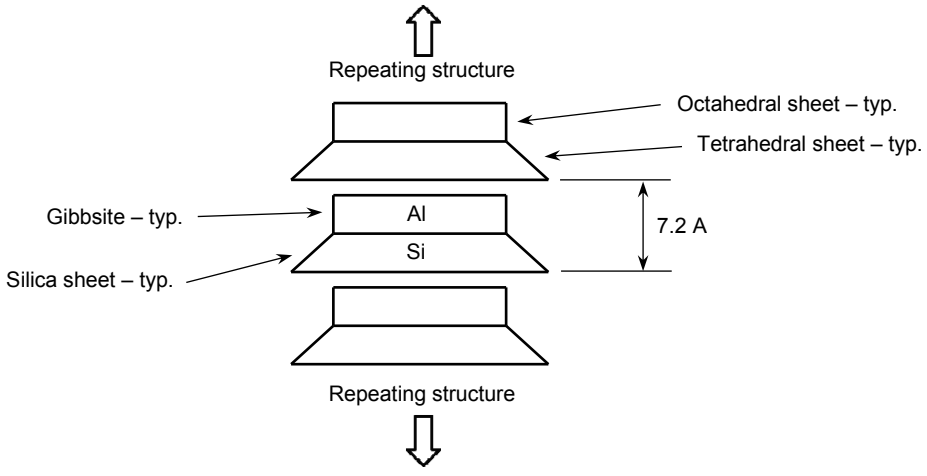

Figure 2.8: Schematic Diagram of Kaolinite (after Lambe, 1953)

2.3.2 Halloysite

Halloysite is another 1:1 clay mineral but differs from Kaolinite due to water entrained between the mineral layers. This hydration results in deformations of the crystal structure and random stacking of the mineral sheets giving it a tubular structure. The water can be removed from the mineral layers by heating or air drying but is irreversible. The Halloysite mineral sheet will not rehydrate upon addition of water to the clay mineral (Holtz and Kovacs, 1981). When hydrated, the clay exhibits a 1 nm spacing of the layers and when dehydrated the mineral layers are 0.7 nm in spacing. Halloysite naturally occurs as small cylinders which average 30 nm in diameter with lengths between 0.5 and 10 micrometers. The cation exchange capacity depends on the amount of hydration, as $2H_2O$ has 5-10meq/100g, while $4H_2O$ has 40-50meq/100g.

2.3.3 Montmorillonite/Smectite

Montmorillonite, or Smectite, is a 2:1 mineral containing two silica tetrahedron sheets and one alumina (gibbsite) octahedron sheet. The octahedron sheet is located between the two silica tetrahedron sheets forming a single layer (Figure 2.9). The tips of the silica tetrahedrons form a bond with the hydroxyls of the alumina octahedrons by Van der Waals' forces. The bonding forces are weak and allow water and exchangeable ions can enter the layers. Typical thickness of a 2:1 mineral layer is approximately 0.96 nm (9.6 A) and extends laterally in both directions indefinitely (Holtz and Kovacs, 1981). Due to the very small size and the affinity for water, Montmorillite is highly expansive

depending on the initial and final moisture contents. The cation exchange capacity of smectite is in the range of 80 to 150 meq/100 gm.

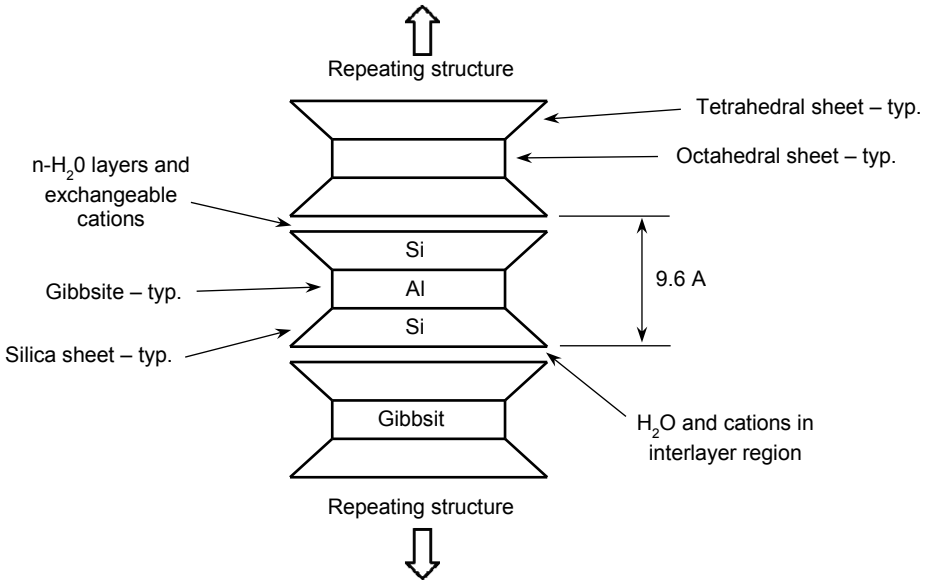

Figure 2.9: Schematic Diagram of Montmorillonite (after Lambe, 1953)

2.3.4 Illite

Illite is another 2:1 mineral similar to Montmorillite with the interlayers bonded with a potassium atom. Illites consist of one octahedral sheet sandwiched between two silica tetrahedral sheets. The potassium atom fits into the hexagonal space created in the silica tetrahedron sheet and bonds the mineral layers together (Figure 2.10). The resulting charge is somewhat balanced by the potassium atoms in the hexagonal space between the layers. This makes the potassium essentially non-exchangeable since bonding is very strong. Ionic substitutions do occur in Illite, usually in the silica tetrahedral layers.

This strong bonding reduces the potential for expansion by preventing water intrusion between the layers allowing the layers to remain essentially constant (Mitchell, 1993). The cation exchange capacity of Illite is in the range of 10 to 40 meq/100 gm.

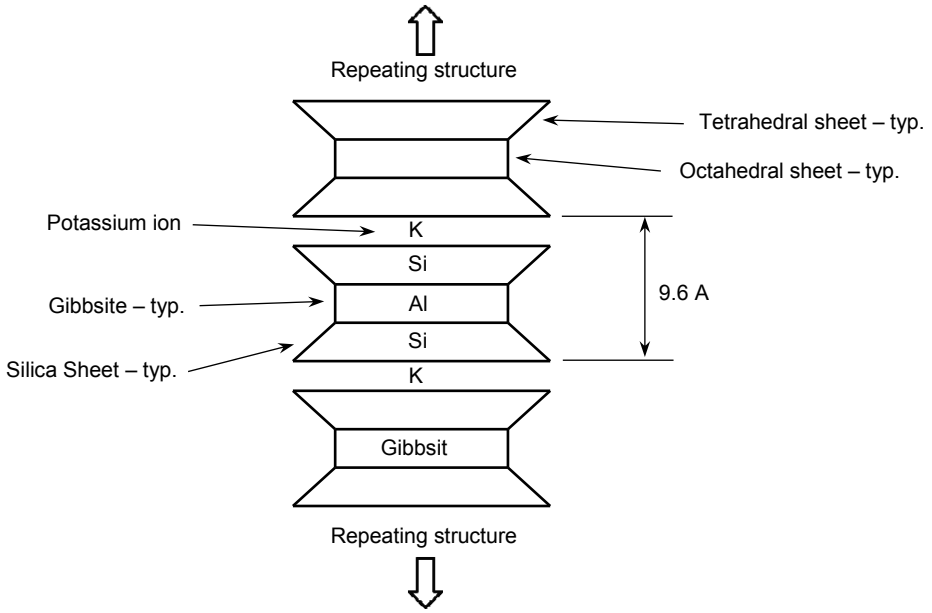

Figure 2.10: Schematic Diagram of Illite (after Lambe, 1953)

2.3.5 Chlorite

Chlorite is a 2:1:1 mineral consisting of a silica tetrahedron sheet, an alumina octahedral sheet, a silica tetrahedron sheet followed by either a gibbsite or brucite sheet (Figure 2.11). Unlike other 2:1 clay minerals, chlorite's interlayer space is made up of Mg2+ or Fe3+, more commonly referred to as the brucite-like layer. Chlorite can be missing an occasional brucite or gibbsite layer and also have considerable isomorphous substitution. This may lead to a higher

susceptibility to swelling due to water entering between the sheets. Generally, it is significantly less active than montmorillonite (Holtz and Kovacs, 1981). Cation exchange capacity for silt size chlorites varies from 4 to 32 meq/100 gm and for −2 μ chlorite particles from 30 to 47 meq/100 gm. Cation exchange capacities for −2 μ and −1 μ chlorites are essentially the same.

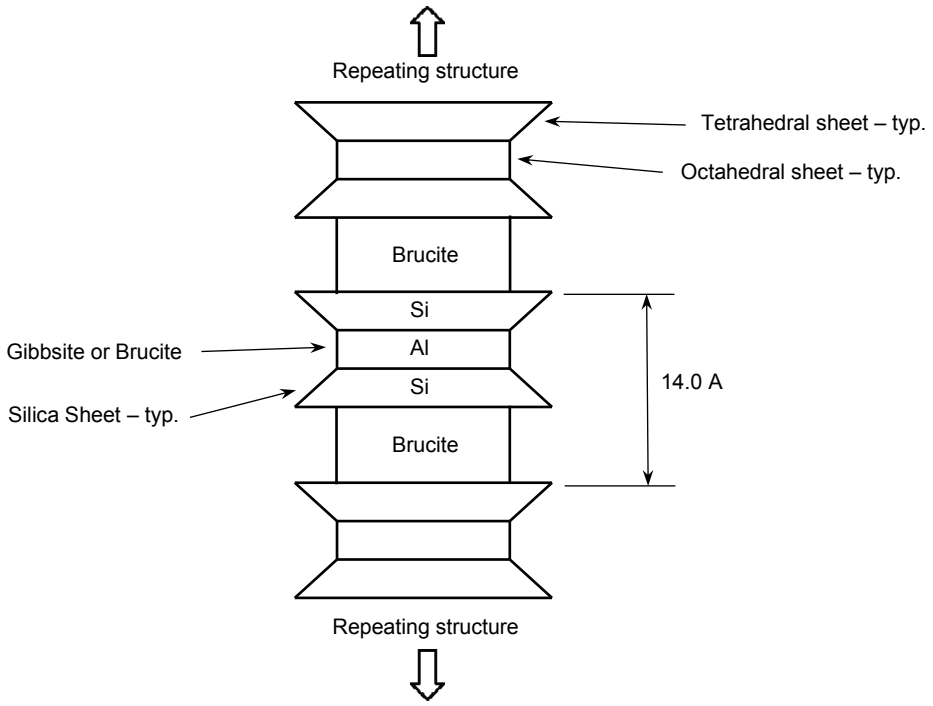

Figure 2.11: Schematic Diagram of Chlorite (after Mitchell, 1976)

2.4 Swelling Potential of Clay Soils

One of the most important considerations in determining risks to structures due to expansive soils is identifying the vertical and lateral swell potential of the soil and the resulting swell pressures. One-dimensional tests are by far the most widely used method to estimate expansive soil swelling potential and pressures. This is due largely to the simplicity of the procedures and the availability of the testing equipment. Standard test methods for evaluating the potential for one-dimensional heave / settlement and swell pressure of cohesive soils is described in ASTM D 4546 (One-Dimensional Swell or Collapse of Cohesive Soils). Three oedometer/consolidometer tests useful for measuring potential swell / settlement and swelling pressure can be described as follows:

1) Free-swell test - A seating pressure (e.g., 0.01 tsf) is applied to the test sample in an oedometer/consolidometer, the sample is inundated with water and allowed to swell vertically until primary swell is complete. The sample is loaded following primary swell until its initial void ratio / height is obtained. The total pressure required to reduce the test sample height to the original void ratio / height prior to inundation is defined as the swell pressure.
2) Overburden-swell test - A vertical pressure exceeding the seating pressure is applied to the test sample in an oedometer/consolidometer and the sample is inundated with water. The test sample may swell, swell then contract, contract, or contract then swell. The vertical pressure is

typically chosen to replicate the in situ overburden pressure and may include structural loads depending on the purpose of the test.

3) Constant-volume swell test - . A seating pressure and additional vertical pressure (typically equivalent to the in situ overburden pressure) is applied to the test sample in an oedometer/consolidometer and the sample is inundated with water. Additional vertical pressure is applied as needed or removed to maintain a constant void ratio / height of the test sample. A consolidation test is subsequently performed and the total pressure required to maintain a constant void ratio / height of the test sample is the measured swell pressure. This measured swell pressure is corrected to compensate for sample disturbance by using the results of the subsequent consolidation test. A suitable correction procedure is similar to that for estimating the maximum past pressure.

The procedures outlined typically use a rigid soil confining ring in an oedometer/consolidometer apparatus to measure the vertical stress and strain components of swell.

2.4.1 Consolidometer Swell Test

ASTM Method D4546, “Standard Test Methods for One-Dimensional Swell or Collapse of Cohesive Soils”, describes three laboratory methods for measuring free swell, swell pressure and the magnitude of one-dimensional swell or collapse of compacted or intact cohesive soils. The test methods can be used to measure the magnitude of one-dimensional wetting-induced swell or collapse (hydrocompression) under different vertical loading, as well as the magnitude of

vertical swell pressure and the magnitude of vertical free swell. It can also be used to obtain data for stress-induced compression following wetting-induced swell or collapse. All of the methods involve the use of a one-dimensional oedometer/consolidometer apparatus to laterally restrain the soil sample and allow for access to free water. Three alternative methods are described to determine the swell behavior and measure the swell parameters of the soil. The three testing procedures for determining the swelling pressure of a soil can be described as:

- Method A – wetting-after-loading testing of multiple samples - differing surcharge loading performed on compacted or natural soil samples followed by inundation with free water.
- Method B – single point wetting-after-loading testing of a single sample – a single surcharge load on a single “intact” specimen of natural soil, or a single “intact” specimen of compacted soil obtained from an existing fill or embankment followed by inundation with free water.
- Method C – loading-after-wetting test – after completion of the Method A or B testing increments of additional vertical loads are applied to the sample and the load-induced deformations are determined. The results would apply to situations where new fill and/or additional structural loads are applied to the ground that has previously gone through wetting-induced heave or settlement.

Typically, two classes of testing are performed, free swell and either a free swell test followed by consolidation or a continuous consolidation upon

inundation of water to keep a constant volume. In the free-swell test, a sample is subjected to an applied load and allowed to swell freely. The resulting final volume changes are plotted against the corresponding applied loads or stresses. The stress corresponding to zero volume change (reloading the sample to the initial void ratio / height) is termed the swelling pressure (Hardy et al, 1962). The swelling pressure may be further defined as the pressure that prevents either a positive or negative volume change.

In the free-swell followed by consolidation or continuous consolidation upon inundation with water, the soil sample is inundated with water and allowed to swell freely with a given load applied. The soil is gradually consolidated back to its original void ratio / height in the conventional manner of a consolidation test procedure. The swelling pressure is defined as the stress necessary to consolidate the specimen back to its original volume or the minimum stress required to prevent swelling (ASTM D4546-08). The swell pressure (Ps) is the applied load required to prevent swell strain (L) divided by the cross-sectional area of the specimen (A):

$$\boldsymbol{Ps = L/A^2} \qquad 2.5$$

Stability is assumed to occur when no further applied load is required to restrict vertical strain.

Swell strain is determined by measuring the resultant heave after reaching stability (no further increase in sample height with time) upon inundation of water

to the sample. The heave is defined as the change in height of the sample and the swell strain in the change in height divided by the initial height of the sample:

$$\varepsilon_v = \frac{\Delta H}{H} \qquad 2.6$$

The test results are commonly plotted as shown in Figure 2.12, vertical height or void ratio versus the log of the vertical load (or stress) applied.

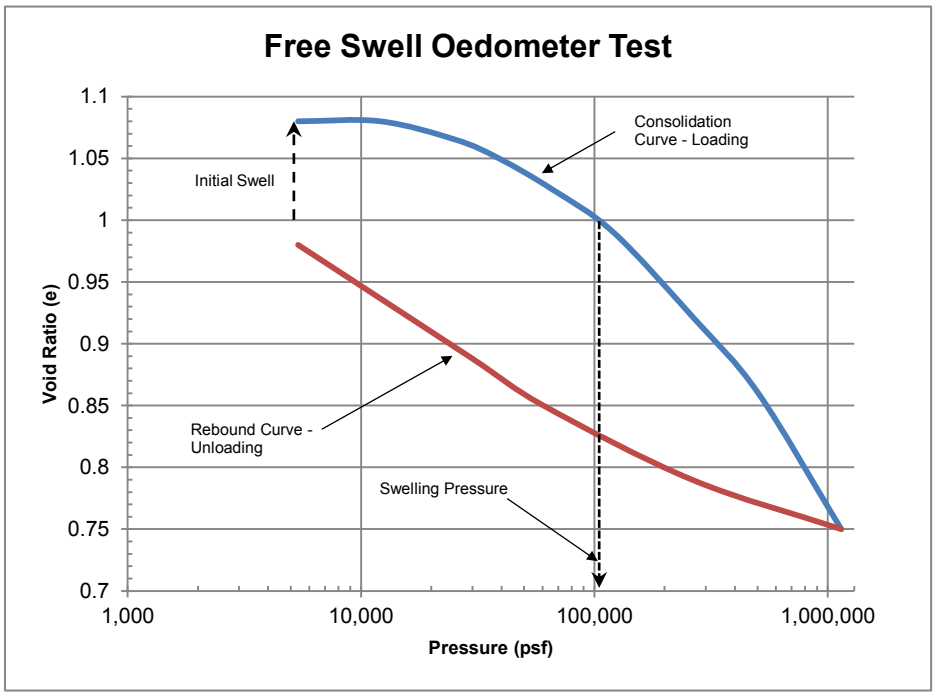

Figure 2.12: Free Swell Oedometer Test Results

The actual stress paths followed during the test can be traced beginning with water inundation initiating the swell of the soil followed by loading of the sample to reach the original height/void ratio. At this point the pressure required (Ps) to resist the swelling can be determined.

To empirically account for sampling disturbance, Fredlund et al. (1980) defined a correction procedure which could be applied to the data to give a corrected swelling pressure. The correction procedure is a modification of the Casagrande type of geometrical construction as shown in Figure 2.13. Using the constant volume oedometer test plot (void ratio versus logarithm of total pressure) a correction can be established by identifying the point of maximum curvature of the curve. The point is found immediately past the uncorrected swelling pressure. From that point, horizontal and tangential lines can be drawn and the resulting angle bisected. The intersection of a line parallel to the rebound portion of the curve and the bisector indicates the corrected swelling pressure.

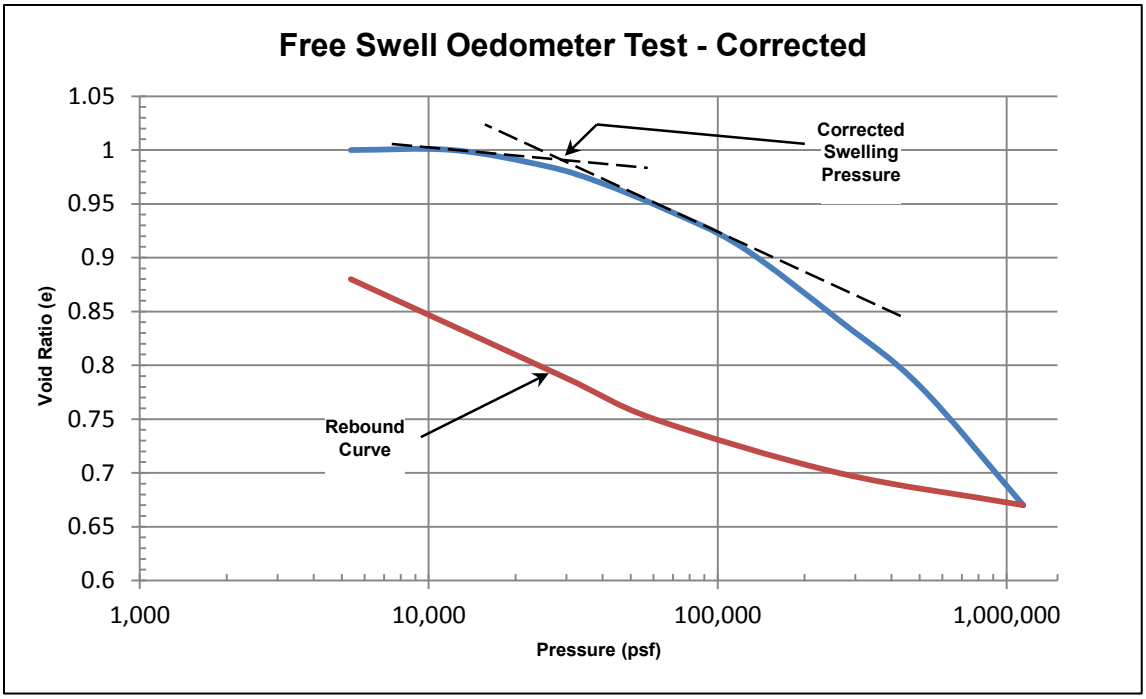

Figure 2.13: Correction for Sample Disturbance (Fredlund, et.al., 1980)

The potential swelling pressure and volume change of a soil sample can be determined from ASTM Method D4546, “Standard Test Methods for One-Dimensional Swell or Collapse of Cohesive Soils”, laboratory tests. The results can be applied to actual foundations with reasonable accuracy when the stress distribution of the foundation soil is understood and the effects of seasonal variations and the movement of moisture beneath the foundation is known. The oedometer tests, in which a soil sample is subjected to estimated surcharge loads, will help understand the in-situ potential expansion and pressure.

3. Lateral Forces on a Foundation

Lateral forces applied to a structural foundation from the surrounding soil are directed so as to apply a load perpendicular to the plane of the wall. This loads the wall in flexure (bending) and it must act as a one-way slab, beam, or two-way slab, depending on the design. Determination of the magnitude and orientation versus the depth of these forces are crucial to the development of a safe and economic design. For a proper structural design, these lateral forces are generated from three sources: the soil used for backfill, the water table depth in the backfill and the surcharge loads (if any) at the top of the backfill in proximity to the wall.

3.1 Lateral Earth Pressure

The magnitude of the lateral soil pressure that can develop in a soil mass is a function of several factors: the type of soil, the strength of the soil, the stress-strain properties of the soil, the unit weight of the soil, the drainage conditions of the soil, the water table depth, and the amount and direction of wall movement when subjected to the lateral soil pressure. In defining the stress-state of the wall three conditions may exist:

(1) The wall is restrained from moving either toward the soil mass or away from the soil mass and the lateral earth pressure on the wall is defined as the at-rest earth pressure. No deformations or displacements are occurring in this stress-state. This is described as an at-rest condition.

(2) The wall may tilt or translate away from the soil mass where a triangular soil wedge, behind and adjacent to the wall, may fail. This lateral earth pressure in this condition is defined as an active earth pressure.

(3) The wall may tilt or translate into the soil mass where, with sufficient movement, a soil wedge may fail. This lateral earth pressure in this condition is defined as a passive earth pressure.

The at-rest earth pressure condition can be explained by means of Figure 3.1, where length A-B is a structural retaining wall that supports a retained soil mass. The backfill is horizontal, typical of a structural basement wall. If the structural wall does not move (rotate) or yield either toward or away from the retained soil, the horizontal lateral earth pressure at any depth to which the wall will be subjected is called the lateral earth pressure at-rest. The total force per unit length of the wall is equal to σ_0.

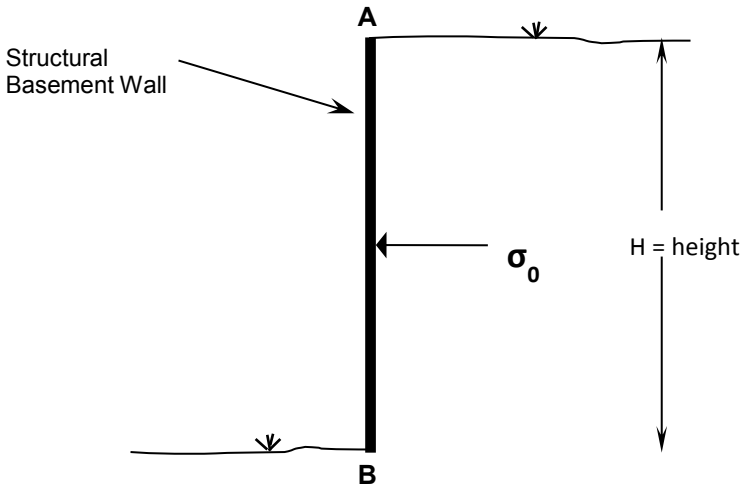

Figure 3.1: At-rest Earth Pressure

If the structural wall tends to move (rotate) or yield away from the retained soil mass, creating a plastic deformation in the soil mass, the lateral earth pressure at any depth to which it will be subjected is called the active earth pressure. This condition is described in Figure 3.2. This active condition can be a result of rotation of the wall about its bottom or top, or by translation of the wall away from the retained soil mass. The resultant force's (σ_a) magnitude, direction, and location per unit length of the wall depends on several factors including soil type, shear strength, backfill incline and stiffness of the structural wall and foundation.

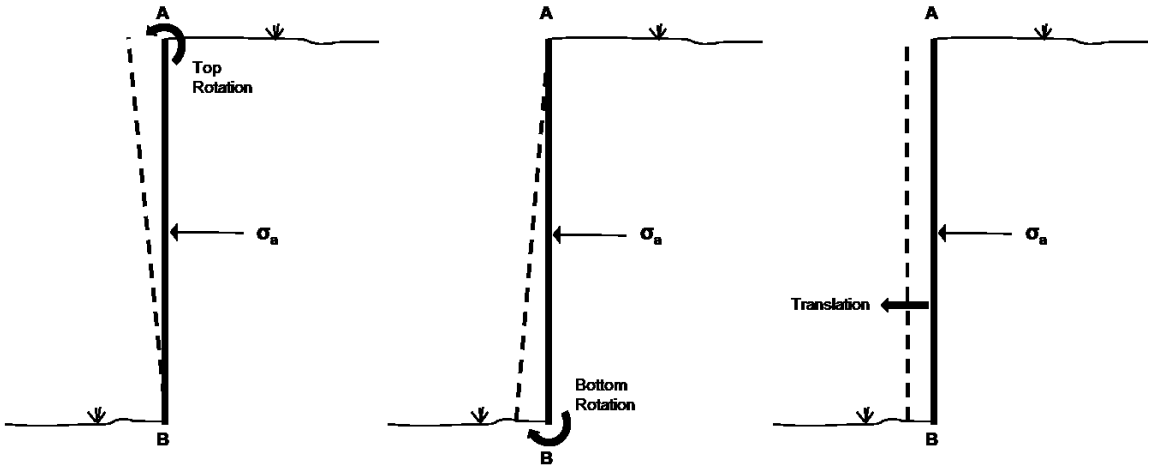

Figure 3.2: Wall Movement for Active Earth Pressure

If the structural wall tends to move (rotate) or yield into the retained soil mass, creating a plastic deformation in the soil mass, the lateral earth pressure at any depth to which it will be subjected is called the passive earth pressure. This condition is described in Figure 3.3. This passive condition can be a result of

rotation of the wall about its bottom or top, or by translation of the wall into the retained soil mass. The resultant force's (σ_p) magnitude, direction, and location per unit length of the wall also depend on several factors including soil type, shear strength, backfill incline and stiffness of the structural wall and foundation.

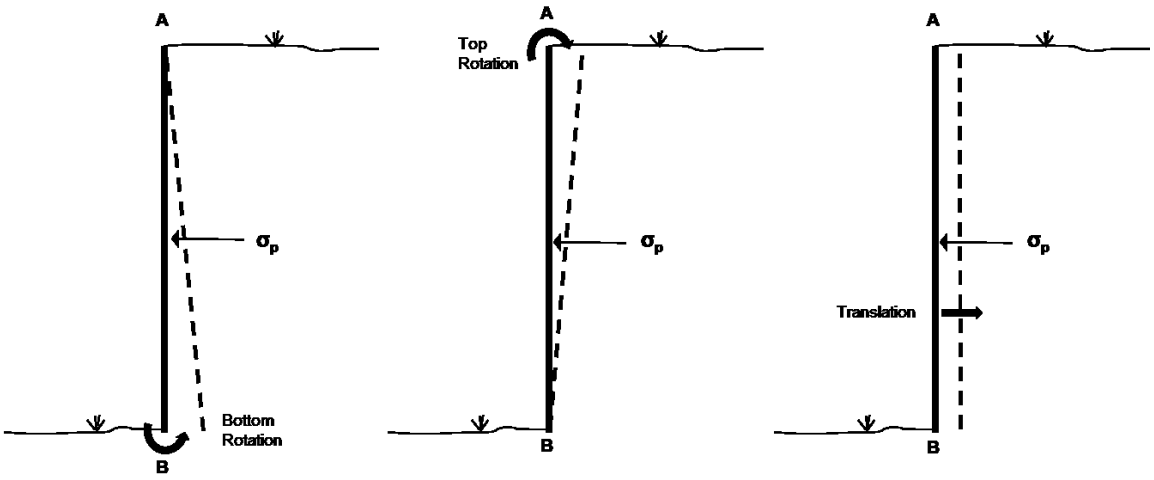

Figure 3.3: Wall Movement for Passive Earth Pressure

In this research the foundation wall is modeled as a two-way slab with sufficient support at the base and top of the foundation wall to prevent either active or passive earth pressures and is therefore modeled using an at-rest earth pressure.

For an at-rest condition, vertical stresses existing in a soil mass at a given depth Z below the ground surface where the water table exists below the depth Z of the soil element is the weight of the overburden and can be written as

$$\boldsymbol{\sigma_v = \gamma_{soil} Z} \qquad 3.1$$

where γ_{soil} is the unit weight of the soil mass for a homogenous, isotropic mass of infinite extent (McCarthy, 1980).

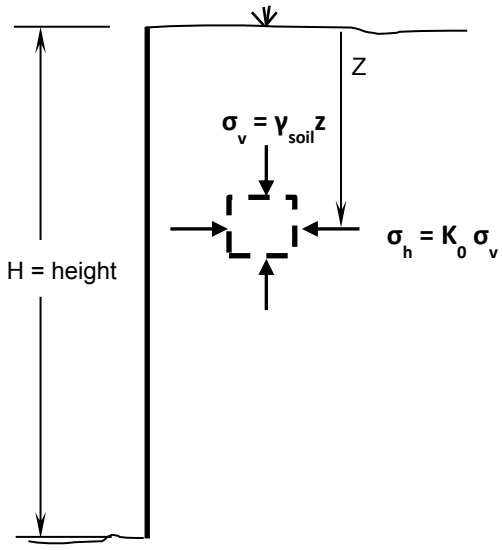

Figure 3.4: Relationship between Vertical and Horizontal Soil Stress

The relationship between the vertical stress and the horizontal stress (Figure 3.4) is determined by calculation of the coefficient of lateral earth pressure at-rest K_0 and is the ratio of horizontal stress σ_h and the vertical stress σ_v.

$$\boldsymbol{K_0 = \frac{\sigma_h}{\sigma_v} = \frac{v}{1 - v} \cong 1 - sin\,\varphi} \qquad 3.2$$

Where v is Poisson's ratio and φ is the angle of internal friction of the soil. The above equation (Jáky, 1944) is an empirical approximation and is defined as the

at-rest condition for normally consolidated sands designated K_0 which can be written:

$$\boldsymbol{\sigma_h = K_0 \sigma_v} \quad 3.3$$

For normally consolidated clays, the coefficient of lateral earth pressure K_0 in the at-rest condition is approximated by Brooker and Ireland (1965) as

$$\boldsymbol{K_0 \cong 0.95 - \sin \varphi} \quad 3.4$$

where φ is the drained peak friction angle of the soil. In addition, Brooker and Ireland experimented with normally consolidated clay soils and determined the value for K_0 may be approximated with the Plasticity Index (PI) as

$$\boldsymbol{K_0 = 0.4 + 0.007PI} \quad 3.5$$

This for a Plasticity Index between 0 and 40 and

$$\boldsymbol{K_0 = 0.64 + 0.001PI} \quad 3.6$$

for a Plasticity Index between 40 and 80.

Where overconsolidated clays are concerned K_0 can be defined as follows:

$$\boldsymbol{K_{0(overconsolidated)} = K_{0(normally\ consolidated)}\sqrt{OCR}} \qquad 3.7$$

Where OCR is defined as the overconsolidation ratio. A soil is described as normally consolidated when the preconsolidation pressure equals the existing vertical overburden pressure (the soil has not experienced anything greater than the current overburden stress). If the preconsolidation pressure is greater than the existing vertical overburden pressure the soil is described as being overconsolidated (the soil had experienced a pressure that is larger than the current overburden condition). The overconsolidation ratio can be determined by the ratio of the preconsolidation stress divided by the existing vertical effective overburden stress

$$\boldsymbol{OCR = \frac{\sigma'_p}{\sigma'_{vo}}} \qquad 3.8$$

where σ'_p is the preconsolidation pressure and σ'_{vo} is the effective vertical overburden pressure (Holtz & Kovacs, 1981). As can be seen from the OCR equation, soils that have an OCR = 1 are normally consolidated ($\sigma'_p = \sigma'_{vo}$), soils that have an OCR > 1 are overconsolidated ($\sigma'_p > \sigma'_{vo}$) and finally a soil that has an OCR < 1 is considered underconsolidated ($\sigma'_p < \sigma'_{vo}$).

Typical values have been tabulated for K_0 and are shown in Table 3.1.

Table 3.1: Typical values of the coefficient of lateral earth pressure, K_0.

Soil Type	K_0
Granular, Loose	0.5 – 0.6
Granular, Dense	0.3 – 0.5
Clay, Soft	0.9 – 1.1 (undrained)
Clay, Hard	0.8 – 0.9 (undrained)

3.2 Ground Water and the Lateral Earth Pressure Coefficient

The discussion of lateral earth pressure from a natural soil perspective is applicable only if the soil remains in the current state and water is not introduced to the system. Since the presence of groundwater and specific groundwater levels can fluctuate over time, the lateral earth pressure coefficient K_0 is not a constant for a soil deposit or for a given time period. One way to address this variability is to express the lateral earth pressure coefficient in terms of effective stress. The equation now becomes

$$\sigma'_h = K_0 \sigma'_v \qquad 3.9$$

This expresses the in situ soil stress state in terms of effective stresses to allow for independence from the presence and level of the groundwater table. If the water table level changes the lateral earth pressure coefficient K_0 remains constant as long as we remain in the current soil layer with a constant density

(Holtz & Kovacs, 1981). The coefficient of lateral earth pressure at rest, K_0, is sensitive to many things including the density of the overlying soil layer(s) and the geologic stress history of the soil itself. Where the soil is completely submerged, soil is below the groundwater table, the intergranular (effective) stress between soil particles is reduced by the magnitude of the water pressure at that specific depth as follows:

$$\sigma'_v = \gamma_{soil} Z - u \qquad 3.10$$

where u is equal to the water pressure at the same depth. The presence of water acts to reduce the amount of load the soil intergranular particles accept by taking on some of the load itself. For a normally-consolidated soil that is located above the groundwater table (water below depth H, Figure 3.5) the lateral at-rest pressure acting against the wall would increase with depth uniformly. The resulting distribution (Figure 3.5) would be represented by a triangle with the maximum pressure existing at the base of the triangle and equal to

$$\sigma_h = K_0 \sigma_{v=} K_0 \gamma_{soil} Z \qquad 3.11$$

and the resultant lateral force per unit of wall length is

$$P_0 = \frac{1}{2} K_0 \gamma_{soil} H^2 \qquad 3.12$$

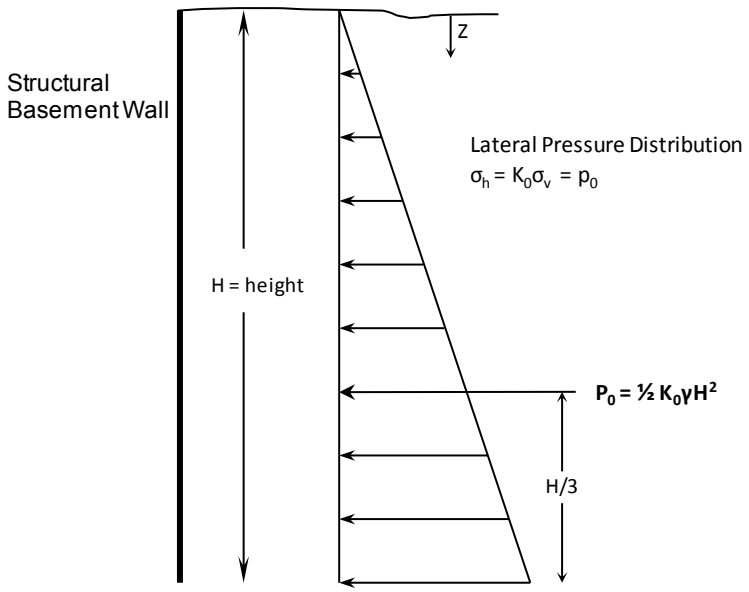

Figure 3.5: Subsurface Stresses – Soil in At-rest Condition

In the case where the soil is below the groundwater table, the intergrannular or effective stress between the soil particles is reduced by the hydrostatic pressure of the water taken at the same depth

$$\bar{\sigma}_v = \gamma_{soil} Z - u = \sigma_v - u \qquad 3.13$$

Where u is the magnitude of the water pressure at depth Z. The net effect of the soil being within the water table (submerged) is that compared to a non-submerged soil given the same conditions, the lateral soil pressure is less.

However, since the soil is located below the water table (submerged) you have to account for the hydrostatic pressure of the water on the wall. The total effect on the wall lateral pressure due to the hydrostatic pressure and the lateral soil pressure imposes a larger total lateral force than a non-submerged soil (Figure 3.6).

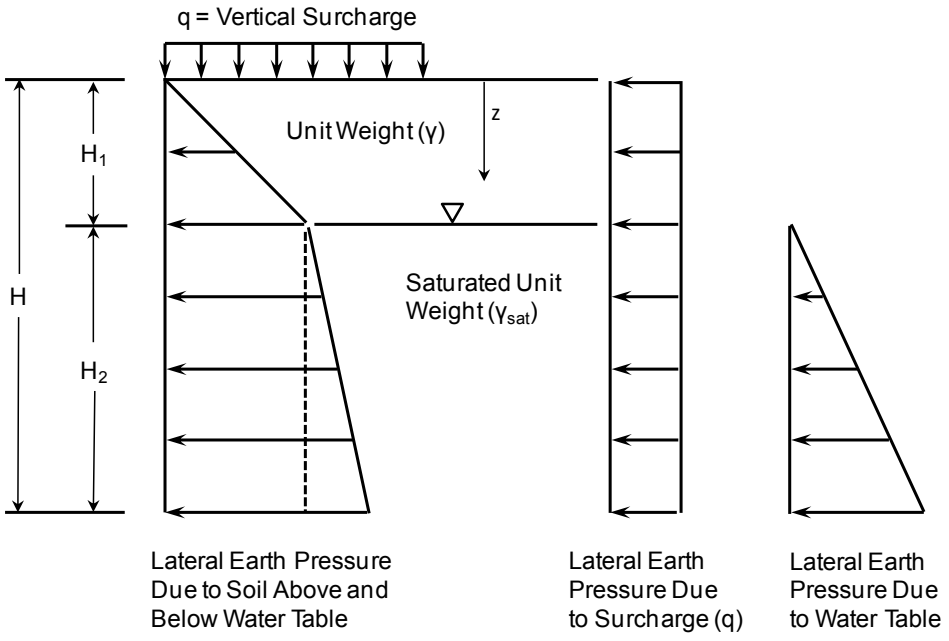

Figure 3.6: Subsurface Stresses – Soil in At-rest Condition with Vertical Surcharge and Influenced by the Water Table

4. Rigid Wall Foundation Design

The purpose of a reinforced concrete basement wall is multifold. It "retains" or holds in place the wall backfill, which tends to push inward on the basement of the structure, and supports the structural loads which typically react vertically. Design information for basement foundations is scattered across multiple sources leaving design engineers to navigate and assimilate the appropriate information for a complete design. Most of the sources used today use prescriptive design practices and are related back to the Unified Soil Classification system for backfill loads. Typically, the design of basement walls uses a combination of the International Building Code (IBC), the International Residential Code (IRC) and the American Concrete Institute's (ACI) 318, *Building Code Requirements for Structural Concrete*.

4.1 International Building Code

The International Building Code (IBC), within multiple sections, outlines a prescriptive approach to basement wall design for walls that are supported at the top (floor diaphragm) and at the bottom (Keyed or doweled into a footing). Section 1610, Table 1610.1 provides soil lateral loads based on the Unified Soil Classification (USC) system. If the top of the wall is restrained from horizontal movement the design uses an at-rest pressure. Surcharge loading is to be included in the analysis and if expansive soils are a concern a note indicates that the lateral pressure may increase. Section 1802 outlines foundation and soils investigations with some discussion on expansive soils.

Section 1802.3.2 outlines the provisions for classifying an expansive soil as follows:

1) Plasticity Index (PI) greater than or equal to 15 in accordance with ASTM D4318
2) Greater than 10% of the soil particles passing a #200 sieve (75uM) in accordance with ASTM D 422
3) Greater than 10% of the soil particles less than 5uM in size in accordance with ASTM D4829
4) The Expansive Index greater than 20 in accordance with ASTM D4829

One caveat is included in the criteria that if #4 is true, the provisions described in #1, #2 and #3 are not required. Section 1804 outlines the load bearing pressure, lateral pressure and lateral sliding resistance capacity for soils (Table 1804.2) using the UCS system. Section 1805.2 outlines footing options and depths and section 1805.5 continues with the foundation wall design for concrete and masonry wall designs. Table 1805.5 (1) provides the minimum wall thickness for plain concrete and plain masonry walls. Tables 1805.5 (2,3,4) provide the vertical reinforcement requirements for 8-inch, 10-inch, and 12-inch wall thicknesses based on an unbalanced backfill and three groupings of soil types based on the UCS system. Included in the table are reinforcement location, grade of reinforcement, minimum concrete strength and alternate sizes of vertical reinforcement available for use. The provision of the code gives the required amount of vertical reinforcement to resist lateral forces or pressures

given a general soil type. The design approach is based on a one-way behavior of the basement wall. The wall acts as a vertical beam pinned at the top and bottom with the beam length equal to the height of the wall and the beam width equal to the length of the foundation wall. No explicit benefit is given to support at corners or bump-outs. The vertical pinned-pinned beam design assumes a triangular soil loading profile, exerting pressure on the exterior surface of the basement wall. The resulting beam reacts in tension on the interior, unsupported wall and compression on the exterior of the beam. Reinforcing steel is prescribed on the interior side of the beam due to the tensile forces present at that location. The footing is assumed to provide no rotational resistance and is designed primarily to resist the gravity loading of the structure and "pinned" by way of the floor. As part of the prescriptive approach, reinforcement requirements are given for various "unbalanced backfill" heights reflecting the amount of backfill being retained. Section 1805.8 addresses foundations in expansive soils but is limited to the design of slabs-on-grade and mitigation of the soils as opposed to the actual design of a structure to resist the forces applied. Section 1907 describes the details of the reinforcement to include hooks, the placement of reinforcement, protection, etc. and primarily references ACI 318 for the actual design details.

4.2 International Residential Code

The International Residential Code, Chapter 4, addresses foundation design for one and two family dwellings. Section R401.4.1 references Table R401.4.1 where presumptive load-bearing values for foundation materials are

given. Values in the table are based on the UCS system. Section R401.4 includes a note to direct soils testing for expansive, compressible, shifting or other unknown soil conditions without any distinct criteria specified. Section 402.2 outlines the minimum specified compressive strength of concrete for the type or location of the concrete construction against the weathering potential for the application. Section R403 continues with the sizing of the footings, described in section R403.1.1, and includes the minimum width of concrete or masonry footings in Table R403.1(1). Expansive soils, as related to the footing, are addressed in section R403.1.8 by referencing the International Building Code (IBC), section 1805.8. It gives the same provisions for classifying an expansive soil as defined in section 1802.3.2 of the IBC, namely testing for the Plasticity Index, soil fines and the Expansion Index. Section R404 outlines prescriptive solutions for the top reactions for a foundation wall based on UCS system for varying soil unbalanced backfill heights (Table R404.1(1)) and the maximum plate anchor-bolt spacing based on unbalanced backfill height using the UCS system (Table R404.1(2)). The section also specifies the maximum aspect ratio (l/W) for unbalanced backfill height based on the UCS system (Table R404.1(3)). Concrete foundation wall minimum vertical reinforcement size and spacing is addressed in Table R404.1(5) and is based on the unbalanced backfill height and the soil classification from the UCS system. Some of the vertical reinforcement design is referenced to the ACI 318 spec. The design approach outlined in the IRC is also based on a one-way behavior of the basement. The wall acts as a vertical beam pinned at the top and bottom with the beam length equal to the

height of the wall and the beam width equal to the length of the foundation wall. Similar to the IBC, no explicit benefit is given to additional support at corners or bump-outs. The vertical pinned-pinned beam design assumes a triangular soil loading profile, exerting pressure on the exterior surface of the basement wall.

4.3 American Concrete Institute

The American Concrete Institute ACI 318 (2005), *Building Code Requirements for Structural Concrete*, does not specifically address the design of basement foundation walls as a single design section. It must be developed through the use of multiple sections. The design process typically begins with the definition of the structural loads outlined in Chapter 9 for various load combinations. Lateral soil loads are not addressed and must be determined using other geotechnical sources. Chapter 14 of the code specifically addresses the design and analysis of concrete walls. The design must satisfy sections 14.2 (general requirements) and 14.3 (minimum reinforcement requirements) plus 14.4, 14.5 or 14.8, which provide design methods (only one of which is used in a given design problem). The shear design of the wall must satisfy requirements in section 11.10 (special provisions for walls) requirements. Vertical and horizontal reinforcement is designed in accordance with Chapter 14, section 14.4 for walls designed as compression members,

All of the design literature requires that the top and bottom of the wall be restrained (pinned) and to satisfy the prescriptive design aids it must act as a pinned-pinned connection. This is accomplished at the base by means of a concrete slab (floor) opposing movement of the base of the wall. In addition, the

top is restrained by the floor diaphragm by means of the connection of the sill plate to the concrete wall, the connection of the sill plate to the floor framing and the framing and stiffness of the floor diaphragm itself.

5. New Foundation Design Approach

Two structural designs were used in this analysis. The first was a rectangular structure (Figure 5.1) that represents a typical two-story, single family home. The structure measures 30 feet on its side by 50 feet in length. The wall maximum height was chosen as 9 feet with a maximum unbalanced backfill height of 8 feet. The thickness of the structural wall was chosen to be 12 inches which meets the International Residential Code's recommendation given backfill conditions, wall height and the soil pressures exerted on the structure. The backfill soil was assumed to be CL at 60 psf, per foot of depth. No allowance was given for granular fill against the structural basement wall or drainage for the soil against the exterior wall.

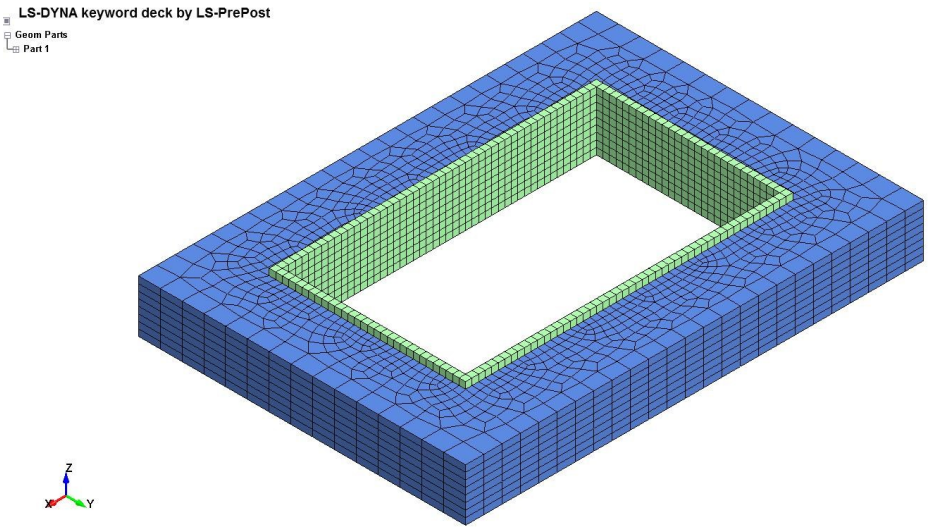

Figure 5.1: Rectangular Structure and Soil Backfill

The second structure was chosen to be a curvilinear structure in the shape of an ellipsoid (Figure 5.2). The minor axis was chosen to be a 15 foot radius and the major axis was chosen to be a 25 foot radius. This was to model the curvilinear structure as close to the same dimensions as the rectangular structure. The same wall thickness of 12 inches was used and the height of the structural wall was also 9 foot high. The soil backfill type, height and drainage was also chosen to be the same as the rectangular structure at CL at 60 psf per foot of depth, 8 foot backfill height and no drainage, respectively.

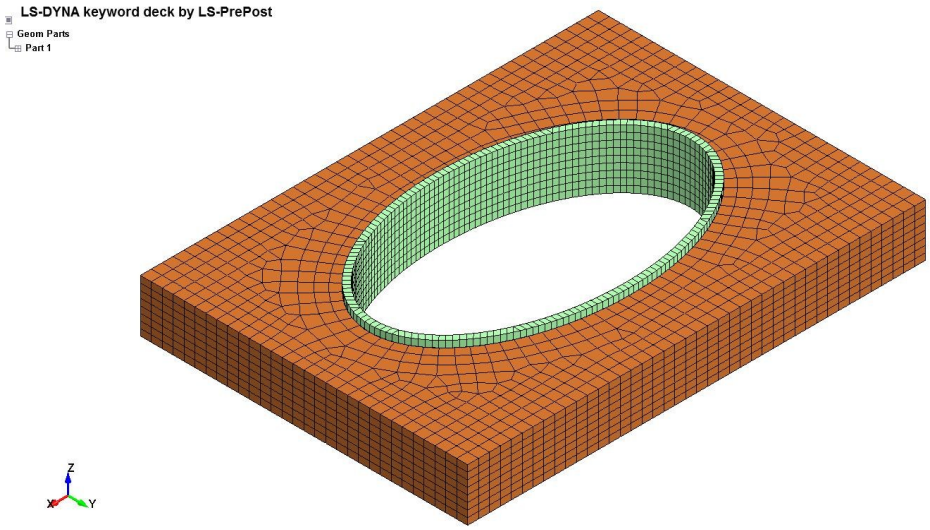

Figure 5.2: Curvilinear structure and soil backfill

The following assumptions were made in the design of the structures:

- Each structure has a full basement floor.
- 3 inches thick and tight against the bottom of the foundation with adequate stiffness to model a pinned joint.

- Joists are used at the top of the wall and connected in such a manner to provide for full-span support of the top of the wall – the top ssurface acts as diaphragm and is the pinned top support for wall.
- The lateral soil loading is identical on all sides of the structure (no unbalanced loading).
- Structure resides in a low seismic region and therefore seismic forces do not control the design.
- The backfill against the structure on all walls is horizontal – no sloped backfill.
- The total service-level vertical load on wall = 1.5 kips/ft.

6. Finite Element Analysis – Foundation

6.1 LS DYNA Model

LS-DYNA is a general-purpose finite element program with the ability to simulate highly nonlinear, transient dynamic finite element analysis using explicit or implicit time integration for complex real-world problems. The software was developed by the Livermore Software Technology Corporation (LSTC), Livermore California. The LS-DYNA code easily handles highly nonlinear, transient, dynamic finite element analysis using explicit time integration. Being a “nonlinear” code it handles changing boundary conditions, large deformations and nonlinear materials that do not exhibit “ideally” elastic behavior. In addition, the code handles “transient dynamic" problems analyzing high speed, short duration events where inertial forces are important. The software code is especially applicable to soil-structural interaction problems involving nonlinear soil materials with potentially large deformations.

LS-DYNA (version 971, Revision 7600.1224) contains numerous concrete material constitutive models that can be used for this analysis. When little is known about the concrete material properties, options to generate material constants given the unconfined compressive strength as an input can be very useful (e.g. MAT 159 CSCM). In this research, MAT Elastic 001 was selected for both the concrete wall and soil due to the ability to define Young’s modulus, the Bulk Density (Rho) and Poisson’s ratio. In addition, high strain rate effects are not needed since loading of the concrete structure is achieved over relatively long spans of time. Since great variability exists in the field when

constructing concrete foundations, defining concrete properties based on finely detailed input parameters is not warranted.

6.2 Model Configuration

The foundation model was fashioned after a “typical” residential concrete foundation designed in accordance with Chapter 4 of the 2006 International Residential Code. The foundation was designed with a wall thickness of 12 inches and a height of 9 feet (108 inches). Two foundation types were modeled, a typical rectangular structure (Figure 6.1) with a length of 50 feet (600 inches) and a width of 30 feet (360 inches) and a curvilinear structure

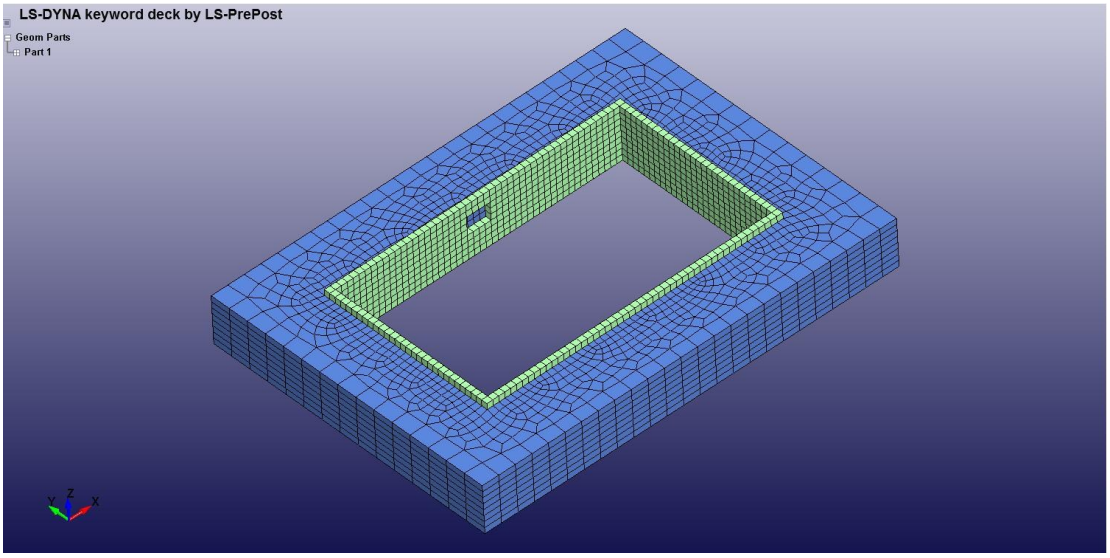

Figure 6.1: Rectangular Structure Finite Element Model

(Figure 6.2) shaped in the form of an ellipse with a major diameter of 25 feet (300 inches) and a minor diameter of 15 feet (180 inches).

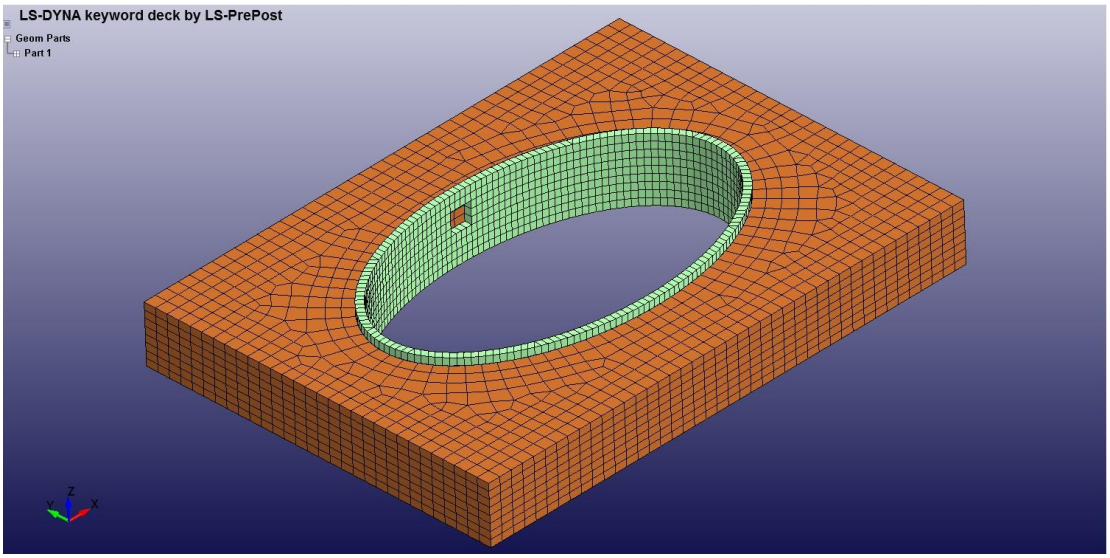

Figure 6.2: Curvilinear Structure Finite Element Model

The curvilinear structure was designed to fit within the same footprint of the rectangular structure. The designs also included an escape window as defined in the 2006 International Residential Code, with a minimum of 5.7 ft^2 opening, 24 inch minimum height and a 20 inch minimum width. The window was placed in the center of the longest wall to evaluate the stress state of the elements around the window. The soil backfill was modeled after a clay soil (Unified Soil Classification System of CH) with a backfill height of 8 feet (96 inches) around the structure with uniform depth of fill around the entire structure. The unbalanced backfill height as defined in the 2006 International Residential Code was calculated as 8.0 ft. The top of the concrete foundation was modeled as a pinned joint, supported by a fixed diaphragm (framed floor) at the top of the wall structure. Motion was restricted in the plane of the wall in the lateral direction but allowed to move relative to the vertical. No rotational limitations

were imposed on the structures. The bottom of the wall was restrained by a continuous 3 inch thick, cast-in-place concrete floor at the base of the foundation. The wall is restrained on the exterior by the soil mass. It was modeled as a pinned joint with rotational freedom at the upper and lower joints. Reinforcement used in the models was based on minimal vertical reinforcement outlined in the American Concrete Institute "Building Code Requirements for Structural Concrete"), Chapter 14. This outlines a minimum spacing of 18 inches on-center for #4 vertical reinforcement. This results in an area of steel of 0.093% for a #4 bar. In the models, the incorporation of reinforcement was accomplished by using the Rule of Mixtures to define the composite properties rather than incorporating discrete beam elements in the model to account for the reinforcement. The models were limited to 10,000 total elements due to the licensing of the LS DYNA software.

6.2.1 Element Types

All models and parts used constant-stress solid brick elements for the concrete foundation and soil backfill material. The LS DYNA default solid element uses a single integration point. In addition, the model used two discrete parts for the concrete structure and the soil backfill.

6.2.2 Loading and Boundary Conditions

Two types of loading were used in the modeling of the concrete foundations, a vertical structural load and an earth-pressure load on the structure. The vertical structural load was applied to the nodes at the top of the

foundation over a time interval of zero to 0.1 seconds and continuing constant to 10 seconds while applying the full vertical load (Figure 6.3).

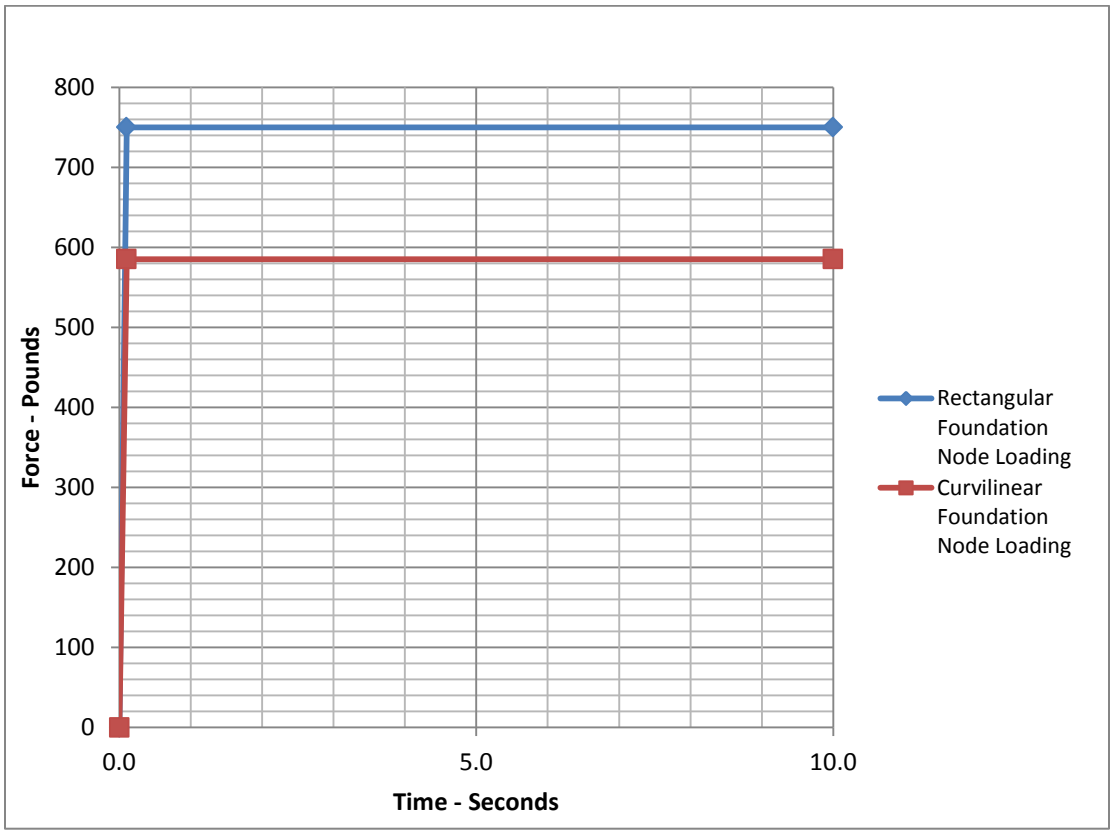

Figure 6.3: Structural Loading of Rectangular and Curvilinear Foundations

The specific load applied to the rectangular foundation nodes was 1500 lb/lf and was determined for each node by the following equation:

$$\boldsymbol{Applied\ Load} = \frac{\mathbf{1500}\ \frac{\boldsymbol{lb}}{\boldsymbol{lf}}}{\frac{\mathbf{312}\ \boldsymbol{nodes}}{\mathbf{156}\ \boldsymbol{lf}}} = \mathbf{750}\ \frac{\boldsymbol{lbs}}{\boldsymbol{node}} \qquad 6.1$$

The specific load applied to the curvilinear foundation nodes was 1500 lb/lf and was determined for each node by the following equation:

$$\boldsymbol{Applied\ Load} = \boldsymbol{1500\ \frac{lb}{lf}} \Big/ \boldsymbol{\frac{332\ nodes}{129.5\ lf}} = \boldsymbol{585.1\ \frac{lbs}{node}} \qquad 6.2$$

The soil loading was accomplished using two approaches.

1. The first was the application of a gravity load to the soil mass surrounding the foundation utilizing the Load_Body_Z card. This imposes a body force due to gravity on the soil mass. The acceleration factor used was 1g or 32.2 ft/s^2 (386.4 in/s^2) in the model.
2. The second soil loading was the application of a lateral load to the soil mass in the X and Y directions to simulate the pressure applied by an expansive soil. The soil mass was extended 10 feet from the foundation walls on all sides of the foundation. This facilitated the placement of lateral loads on the structure in the X and Y directions which was important for the load application on the foundation walls. The applied load in both the X and Y directions was 5,000 psf.

Both loading conditions were applied from zero load to max loading at 4.0 seconds and continuing constant to 10 seconds to ensure stability of the loading (Figure 6.4).

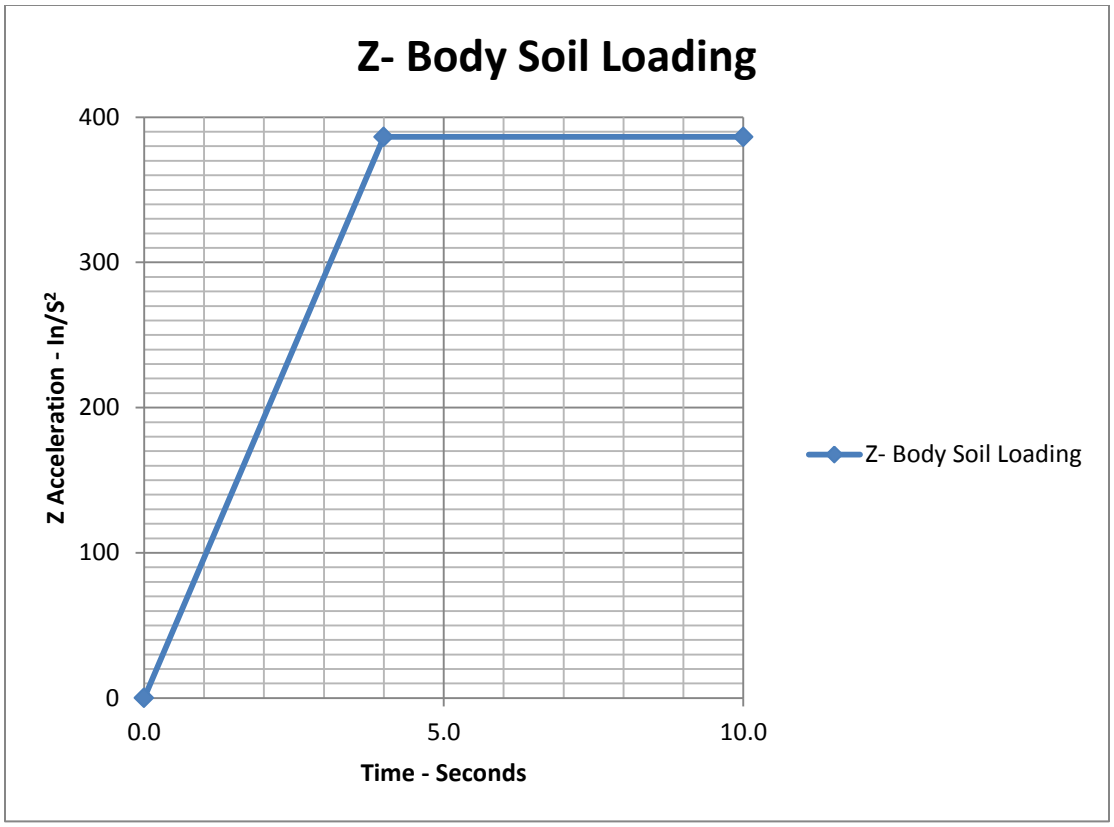

Figure 6.4: Z Body Soil Loading

The boundary conditions used for the models included constraining translational movement (X, Y and Z directions) for all of the soil and concrete foundation nodes located at the bottom of the models. This ensures that the foundation and soil cannot move due to the applied loading. In addition, the top of the concrete foundation was constrained in the X and Y direction to model the Joists used at the top of the wall and connected in such a manner to provide for full-span support of the top of the wall – the joists and floor acts as diaphragm and is the pinned top support for wall.

6.2.3 Contact Type

LS DYNA defines a contact by identifying (using parts, part sets, segment sets, and/or node sets) what is to be checked for potential penetration of a slave node through a master segment. To accomplish this, LS DYNA searches for penetrations, using a number of different algorithms, at each time-step throughout the analysis. When a penetration is found (penalty-based contact) a force proportional to the penetration depth is applied to resist, and ultimately eliminate, the penetration. In this analysis a two-way treatment of contact was chosen between the concrete wall and soil. This type of contact calls the subroutines twice which checks the slave nodes for penetration the first time and checks the master nodes for penetration through the slave segments the second time. The treatment is therefore symmetric and the definition of the slave surface and master surface is arbitrary since both are called in the subroutine and the results end up the same. This results in an increase of computation time due to the extra subroutine calls.

The interface between the concrete wall and soil was modeled using the Surface_To_Surface contact card. The objective of the contact definition is to eliminate any penetration between the interfacing surfaces. The Slave Segment Set and Master Segment Set were set up to use the Part I.D. with the Master defined as the Soil. The Static Friction coefficient was defined as 0.4 and the Dynamic Friction coefficient was defined as 0.2 (ETL 1110-3-446, 1992, Department of the Army). The friction coefficients were based on a wet clay soil against a “troweled” concrete surface. This is a reasonable assumption since

concrete forms are smooth and similar to a troweled surface. There is general agreement on these values in the existing literature although the friction coefficients are dependent on the type of clay, moisture content, density and the relative surface condition of the concrete.

6.2.4 Material Properties

The concrete properties used for this analysis were based on a normal concrete with a compressive strength of 3000 psi, density of 150 lb/ft^3, Poisson's Ratio of 0.16 and a Modulus of Elasticity of 3.146 x 10^{6}psi. In addition, the reinforcing steel used in the model had a minimum yield strength of 60,000 psi and a Modulus of Elasticity of 29 x 10^6 psi.

The soil properties used for this analysis was based on a clay soil (Unified Soil Classification System - CH) with a Unit Weight of 100 lb/ft^3, a Density of 1.498 x 10^{-4} lb/in^3, a Modulus of Elasticity of 2175 psi and a Poisson's Ratio of 0.3.

Table 6.1: LS DYNA model material properties

Material Name	Rho (lb/in^3)	Young's Modulus (lb/in^2)	Poisson's Ratio
Concrete/Steel Composite	2.247E-4	3.146E+6	0.16
Soil	1.498E-4	2.175E+3	0.30

The concrete/steel properties were further combined to generate a composite material using the Rule of Mixtures (Callister, 2001). The Rule of Mixtures asserts that the properties of the combined material are a combination of the individual components of the individual materials. Typical composites have two phases consisting of a matrix (continuous) phase and a dispersed (particulates, fibers) phase. The properties of the composite depends on the specific properties of the phases, the geometry of dispersed phase (particle size, distribution, orientation) and the amount of each phase in the composite. Composites are typically classified as particle-reinforced (large-particle and dispersion-strengthened) composites, fiber-reinforced (continuous (aligned) and short fibers (aligned or random) composites and structural (laminates and sandwich panels) composites. The rule of mixtures calculates an upper limit of the elastic modulus of the composite in terms of the elastic moduli of the matrix (E_m) and the particulate (E_p) phases by the equation:

$$\boldsymbol{E_c = E_m V_m + E_p V_p} \qquad 6.3$$

where V_m and V_p are the volume fraction of the two phases. The calculated composite elastic modulus for a 12 inch thick foundation wall with #4 reinforcement spaced at 18 inch on-center is:

$$E_{composite} = E_{conc}\left(\frac{V_{conc} - V_{steel}}{V_{total}}\right) + E_{steel}\left(\frac{V_{steel}}{V_{total}}\right) \quad 6.4$$

The resulting Modulus of Elasticity for the composite material used in the model was 3,150 ksi.

7. Results

7.1 General Behavior of the Foundation Structures

A review of the structural behavior of the rectangular foundation indicates the model is behaving as a pinned-pinned structural wall with combined vertical and horizontal loading. As shown in Figure 7.1, the deformed shape shows rigidity at the corners with a corresponding lack of displacement. It also shows the greatest displacement at the center of the longest walls exhibiting bowing to the interior due to the lateral pressure from the soil mass. The shape of the deformation in Figure 7.1 is exaggerated (5X displacement factor) to visually demonstrate the deformations.

.

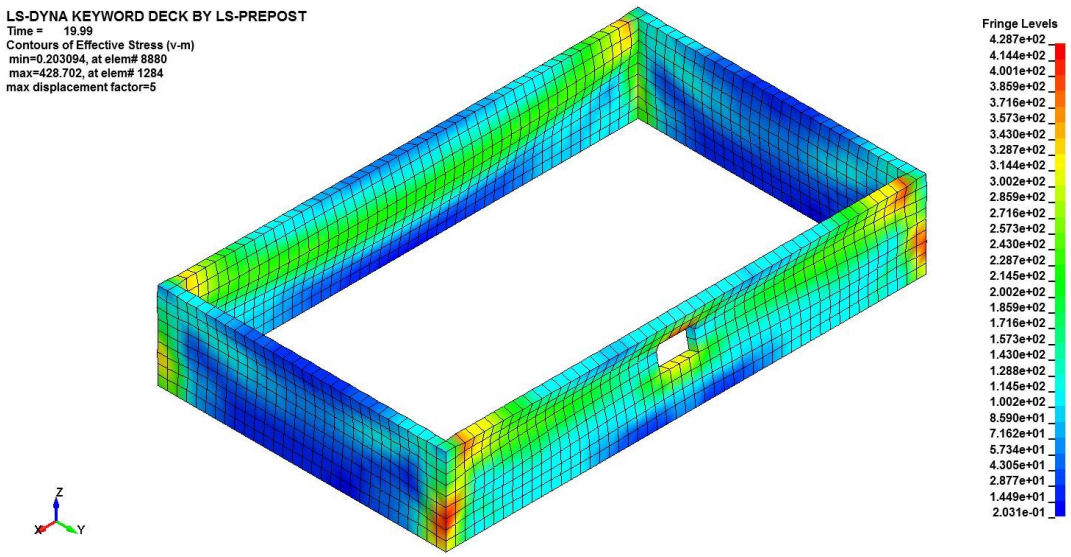

Figure 7.1: Deformed Rectangular Basement Structure (5X Displacement Factor)

Comparing the deformations of the rectangular foundation wall with that of the curvilinear foundation (Figure 7.2) under the same loading conditions, very

little deformation along the entire wall (5X displacement factor) is observed. The load acts in a nearly radial direction and is distributed semi-uniformly around the periphery of the structure. Truly radial forces acting on a circular cross-section result in only compressive forces on the section. There are no bending forces in a completely circular section unless there is a discontinuity such as a window or door. The modeled curvilinear structure capitalizes on this loading advantage by balancing constructability and space utilization of the structure with a shape that takes advantage of compressive forces to increase the load capacity of the structure.

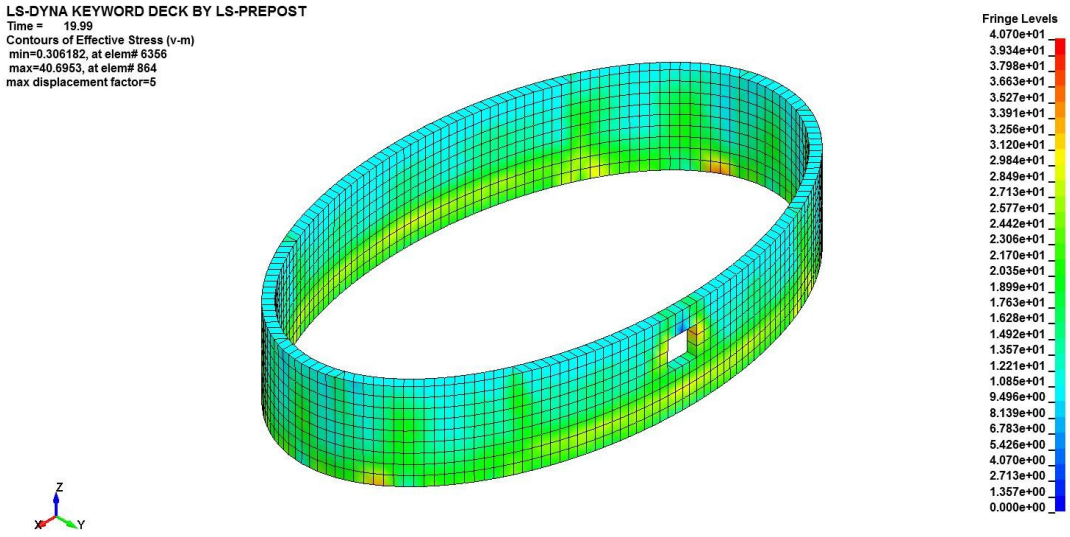

Figure 7.2: Deformed Curvilinear Basement Structure (5x Displacement Factor)

The finite element model indicates that a nearly compressive shape can easily be applied to basement foundation design.

7.2 Wall Displacements of the Foundation Structures

The results of the finite element analysis demonstrate a considerable difference in the mid-wall, out-of-plane lateral displacements between the rectangular basement wall and the curvilinear basement wall (Figure 7.3).

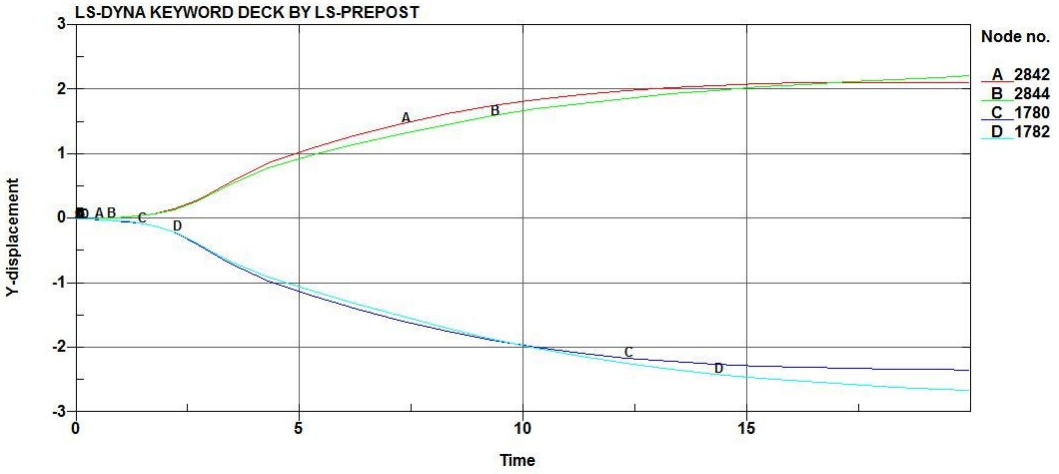

Figure 7.3: Lateral Deflection of Rectangular Basement Structure

The maximum displacement experienced by the rectangular wall was 2.67 inches inward at the top of the window. Similarly, the corresponding node on the opposite wall (without window) shows a deflection of 2.23 inches which was the second greatest deflection in the model. The magnitudes of all four elements analyzed at the mid-span of the longest wall were very similar as shown in the fringe plot of the rectangular structure (Figure 7.4).

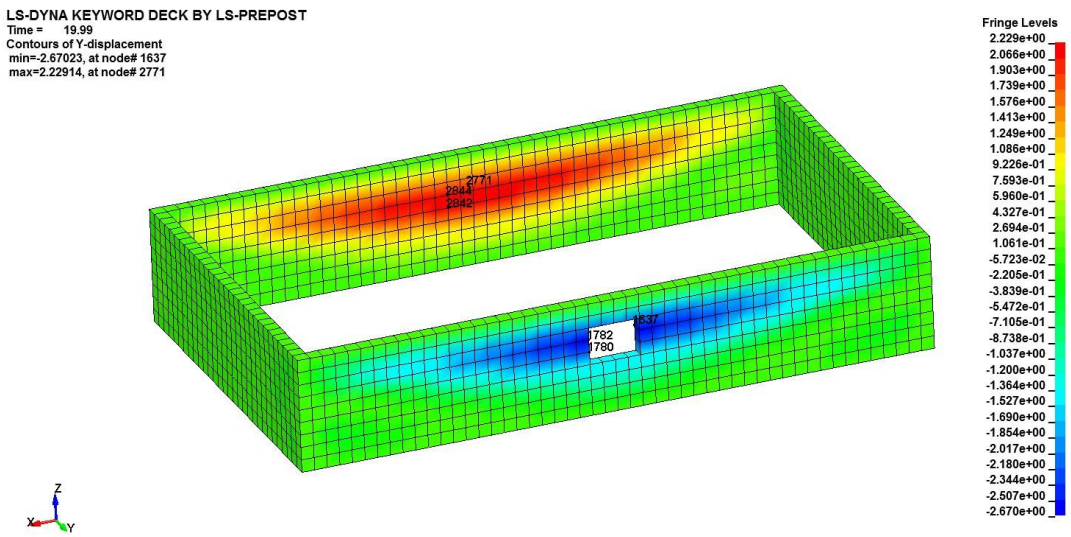

Figure 7.4: Lateral Deflection of Rectangular Basement Structure – Fringe Plot

Comparing the results of the rectangular wall design to the curvilinear wall design there are differences to note. The deflections are essentially zero inches (Figure 7.5) for mid-span elements at the window and on the opposite wall of the curvilinear structure. These locations are representative of the same locations analyzed for the rectangular structure.

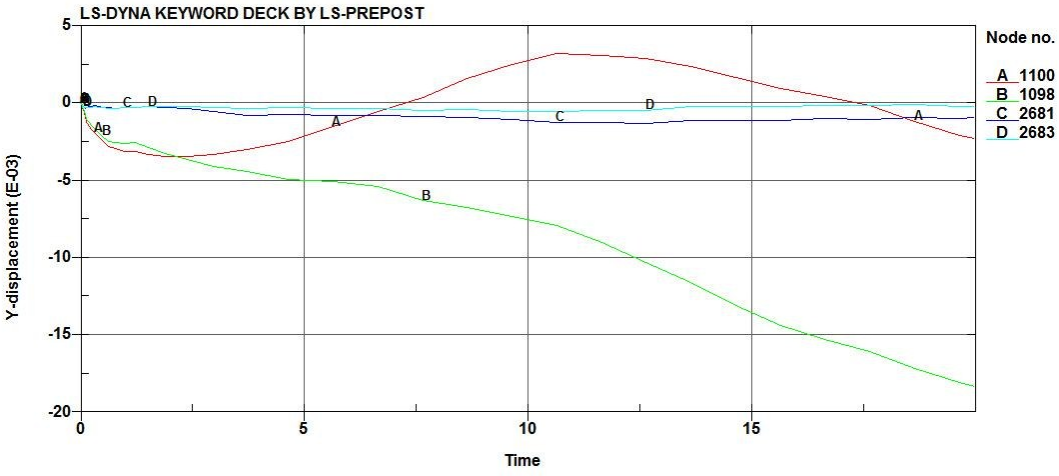

Figure 7.5: Lateral Deflection of Curvilinear Basement Structure

All of the displacements within the curvilinear structure were less than 0.1 inches, an order of magnitude less than the rectangular structure (Figure 7.6).

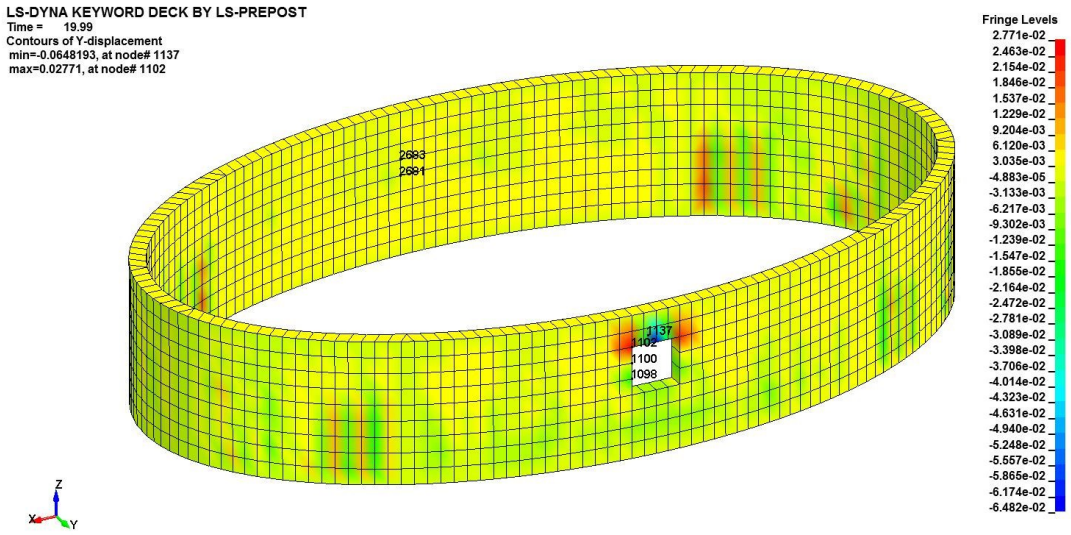

Figure 7.6: Lateral Deflection of Curvilinear Basement Structure – Fringe Plot

It was also noted that the maximum deflections were located along the top of the window, similar to the rectangular structure, although all deflections were below 0.1 inches.

7.3 Vertical Stress State of the Foundation Structures

In addition to the deflection of the walls, the stress state of each foundation type was analyzed. The Z-direction stress (vertical plane of the wall) in the area of the window was analyzed between the two wall designs. The results of the rectangular wall structure indicate a compressive stress of -12 psi and -8 psi in the two elements above the window and increasing larger stresses from 0 psi at the window sill to 66 psi at the bottom of the foundation, all in tension (Figure 7.7).

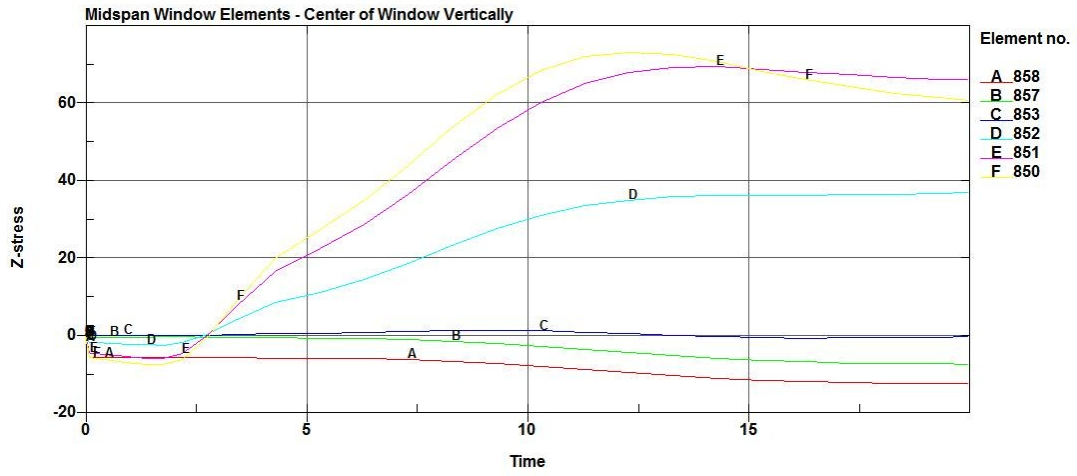

Figure 7.7: Z-Stress (Vertical) Plot of Window Area of Rectangular Foundation

The maximum stress in the rectangular structure is 412.9 psi in tension (Figure 7.8). This occurs at the lower corners of the foundation.

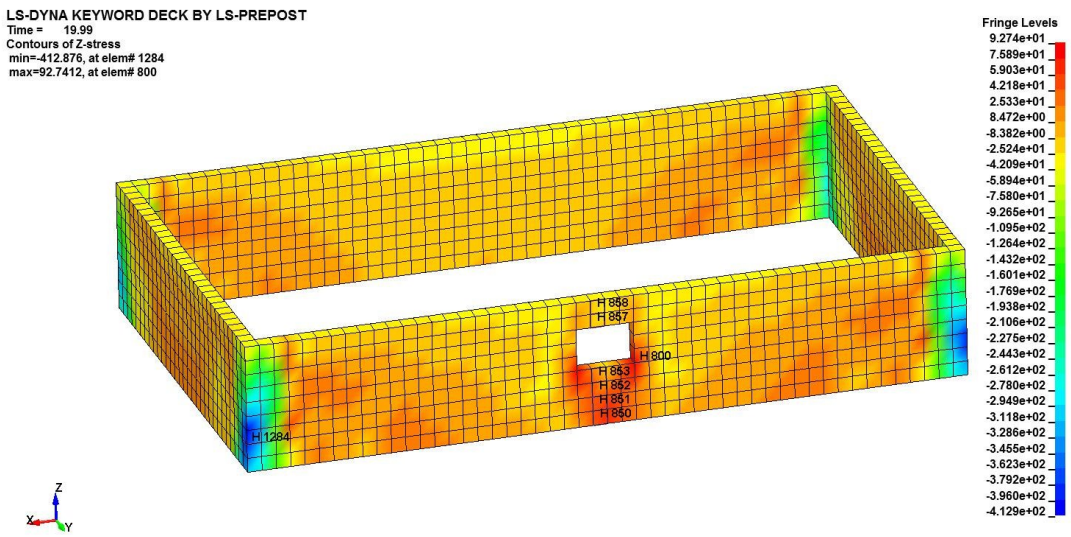

Figure 7.8: Z-Stress (Vertical) of Window Area of Rectangular Foundation – Fringe Plot

Comparing the results of the rectangular wall design to the curvilinear wall design the wall stresses are smaller in magnitude with a maximum stress for the Elements at the window opening ranging from -10.9 psi to 1.8 psi (Figure 7.9).

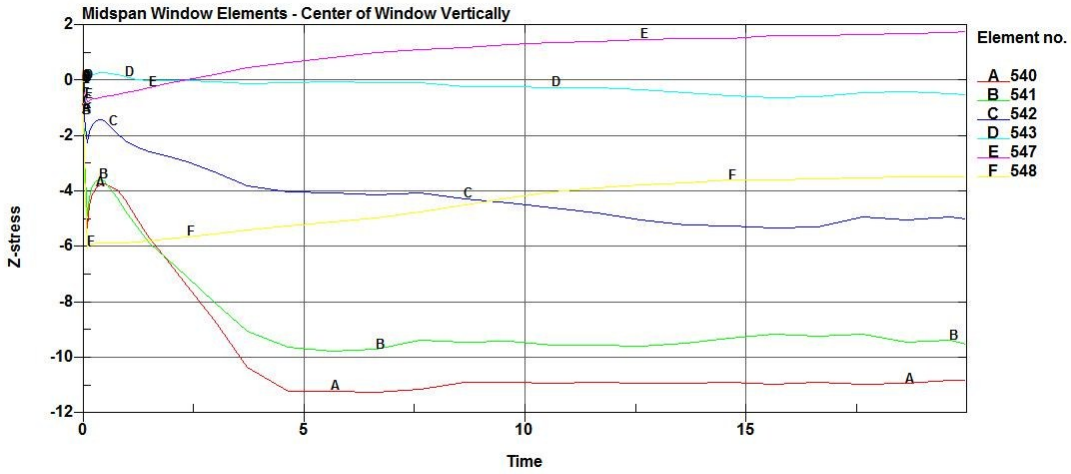

Figure 7.9: Z-Stress (Vertical) Plot of Window Area of Curvilinear Foundation

In addition, the curvilinear structure has a maximum stress at -38.2 psi located at the upper right side of the window cut out. Of greater interest is that all of the vertical stresses in the curvilinear structure are compressive stresses (Figure 7.10) with the exception of element #547 at the top of the window opening. The greatest tensile stress is 1.9 psi which is a significant difference from the rectangular wall design.

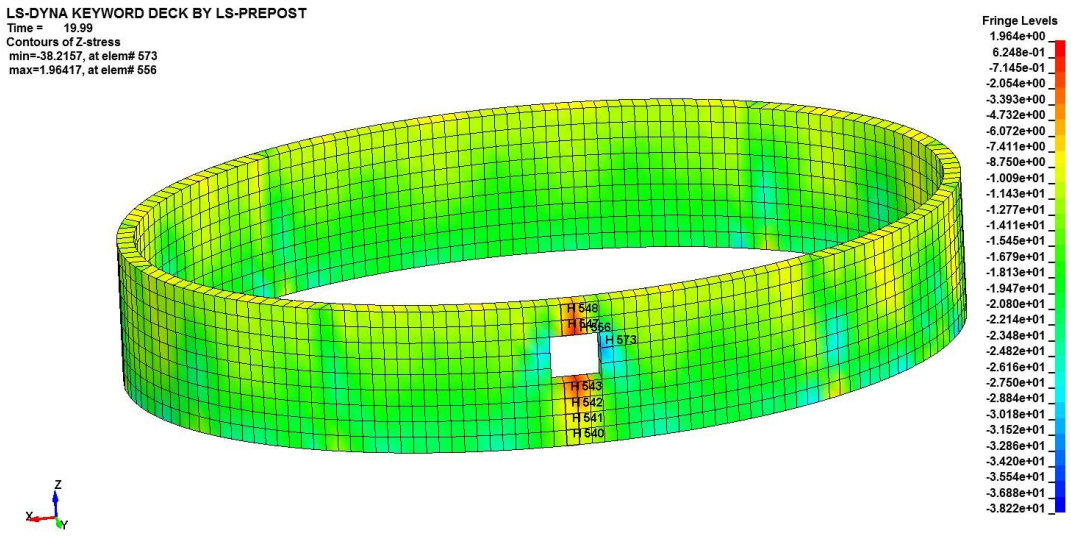

Figure 7.10: Z-Stress (Vertical) of Window Area of Curvilinear Foundation – Fringe Plot

7.4 Shear Stress State of the Foundation Structures

The shear stress for the rectangular structure was evaluated against the curvilinear structure. The greatest shear stress in the rectangular structure was determined to be 235.4 psi (Figure 7.12) located toward the upper corner of the structure.

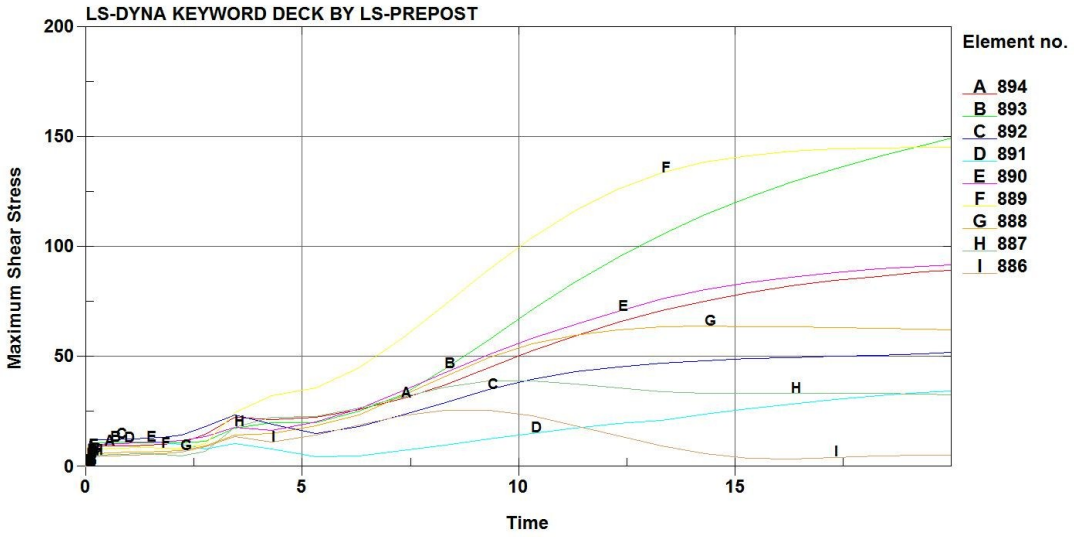

Figure 7.11: Shear Stress Plot along Window Area of Rectangular Foundation

The highest shear stresses are located in the corner areas where the walls transition from X to Y directions. The lowest shear stress in the rectangular structure was 1.8 psi located on the upper side-wall of the rectangular foundation.

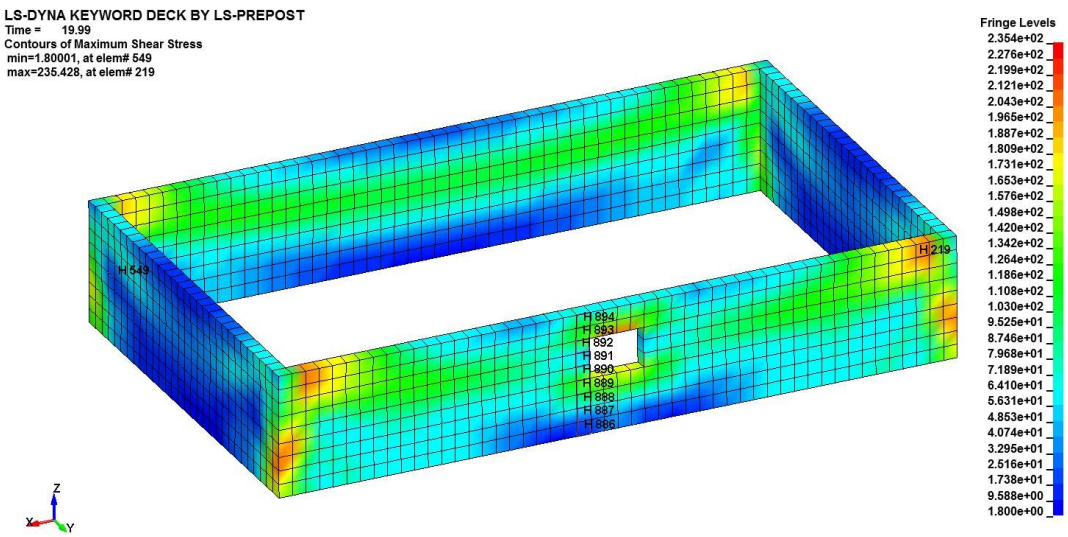

Figure 7.12: Shear Stress along Window Area of Rectangular Foundation – Fringe Plot

Comparing the rectangular foundation to the curvilinear foundation the maximum shear stress for the curvilinear structure is 21.2 psi (Figure 7.14) located along the bottom side of the foundation while the minimum shear stress is 1.4 psi and is located above the window.

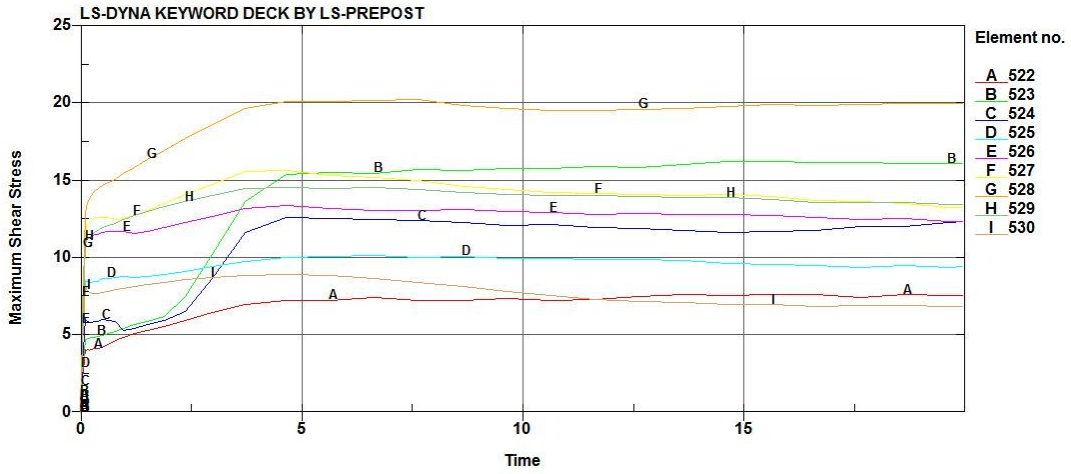

Figure 7.13: Shear Stress Plot along Window Area of Curvilinear Foundation

The difference between the maximum shear stress in the rectangular structure and the curvilinear structure is approximately a factor of ten with the highest shear stresses exhibited in the rectangular structure.

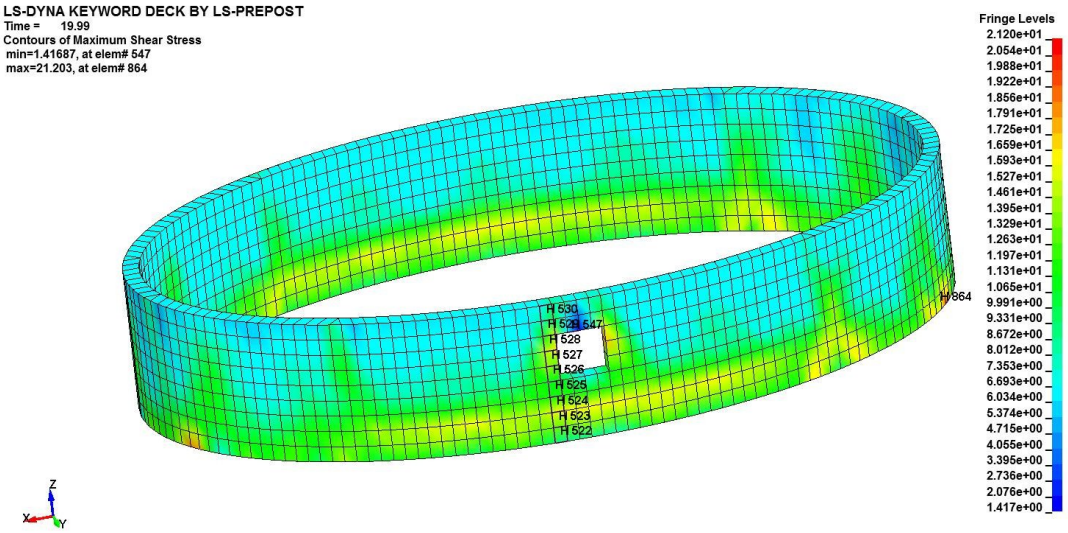

Figure 7.14: Shear Stress along Window Area of Curvilinear Foundation – Fringe Plot

8. Discussion of Analyses Results

Results from the analyses of the rectangular and curvilinear structural designs were analyzed and compared to determine the performance advantages of a curvilinear foundation in environments with high lateral soil loading in addition to the vertical structural loading. This included comparing the lateral displacements of the walls, the vertical stress performance, the shear stress performance and the stress concentration distribution around a discontinuity (window) in each design with combined vertical and horizontal loading.

8.1 Displacements of Foundations

The first observation regarding the lateral deflection of each design was the lateral displacements of the rectangular wall design were greater than 100X of the displacements for the curvilinear design for the same locations. Both foundations experienced the greatest lateral deflections at mid-wall of the long span section of the foundation. Four locations were studied for each design, two around the window and two opposite the window on the solid, continuous long wall.

Table 8.1: Lateral displacement (in) of Rectangular and Curvilinear Wall Designs

Y Wall Displacement Results			
Structure	Node ID	Displacement (in)	Description
Rectangular	Node 1780	-2.3	Lower window
	Node 1782	-2.7	Upper window
	Node 2842	2.1	Lower Adjacent Wall
	Node 2844	2.2	Upper Adjacent Wall
Curvilinear	Node 2681	-0.0009	Lower Adjacent Wall
	Node 2683	-0.0002	Upper Adjacent Wall
	Node 1098	-0.018	Lower window
	Node 1100	-0.0023	Upper window

This is a significant performance difference between the two structural designs and would be advantages from a concrete cracking performance standpoint. This might also have the added advantage of using less reinforcing steel in the design providing better economy of construction, although this would have to be further modeled and analyzed. In addition, the maximum displacement for the rectangular foundation occurred at the right, upper corner of the window at node 1637 and measured 2.67 inches while the maximum displacement for the curvilinear structure occurred at node 1137 and measured 0.06 inches at a location above the window (Figures 8.1 and 8.2).

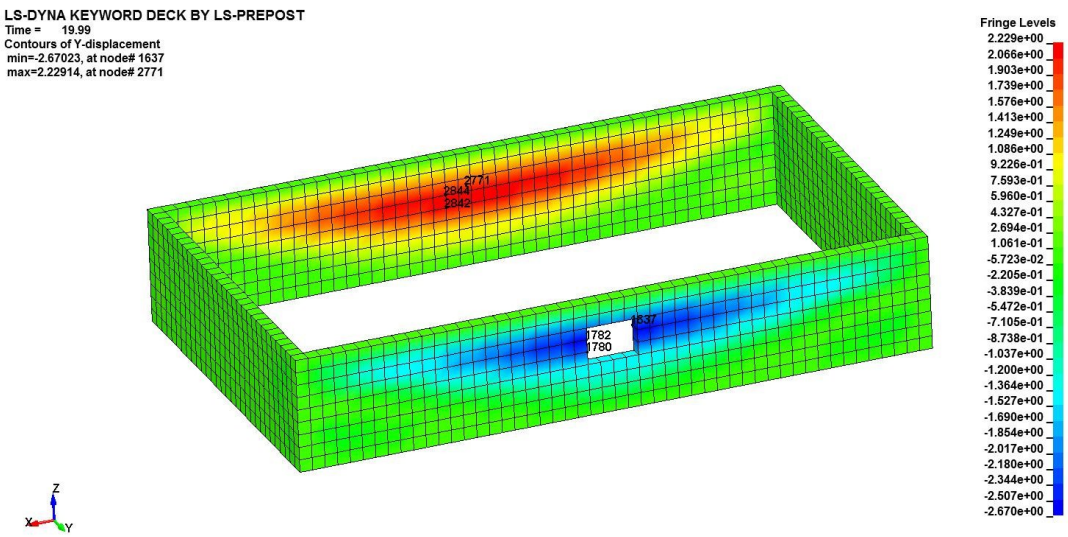

Figure 8.1: Lateral Deflection of Rectangular Basement Structure – Fringe Plot

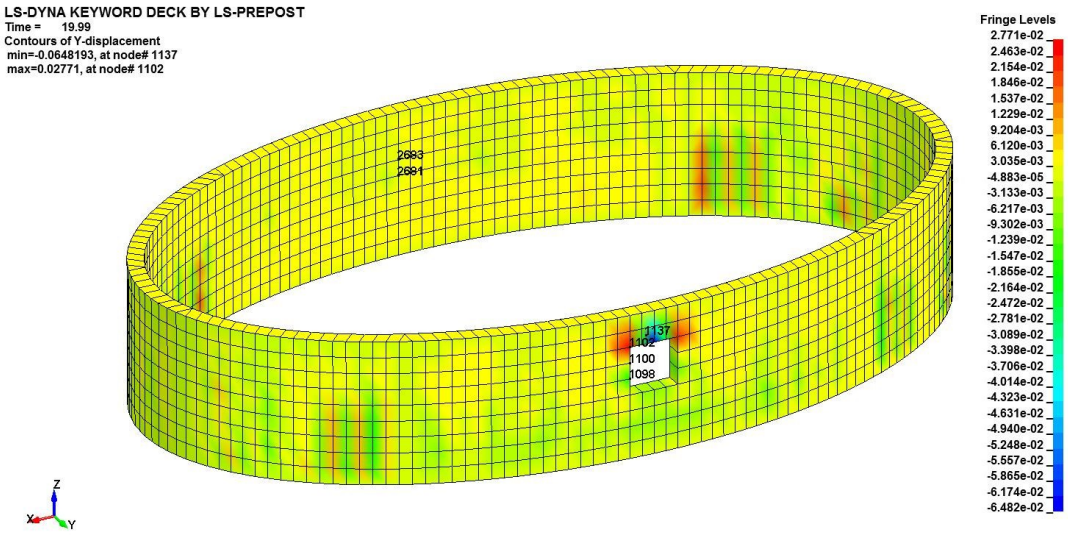

Figure 8.2: Lateral Deflection of Curvilinear Basement Structure – Fringe Plot

The results of the lateral displacement analysis demonstrates that the curvilinear foundation design is a much better design regarding lateral deflections

under combined vertical and lateral loading. All of the deflections for the curvilinear structure were much smaller than the rectangular design with worst-case deflections of the rectangular structure 100 times the magnitude of the curvilinear design.

8.2 Vertical Stress of Foundations

In addition, the vertical stress performance was analyzed in both the rectangular and curvilinear models. A section of wall was analyzed through the depth of the wall located in the middle of the window opening. The results of the analysis demonstrate that the rectangular structure experiences both tensile and compressive forces within the structure due to the combined vertical and lateral loading (Table 8.2). The top of the foundation remains in compression above the window opening and at the window sill, while the bottom of the foundation below the window remains in tension.

Table 8.2: Vertical Stress of Rectangular and Curvilinear Wall Designs

Z Stress Results			
Structure	Element ID	Stress (psi)	Description
Rectangular	Element 858	-12.2	Top of Foundation
	Element 857	-7.2	
	Element 853	-0.2	
	Element 852	37.1	
	Element 851	66.2	
	Element 850	60.9	Bottom of Foundation
Maximum Z-stress in structure		-412.8	
Curvilinear	Element 548	-3.5	Top of Foundation
	Element 547	1.8	
	Element 543	-0.5	
	Element 542	-5	
	Element 541	-9.5	
	Element 540	-10.8	Bottom of Foundation
Maximum Z-stress in structure		-38.2	

Comparing the performance of the rectangular structure to the curvilinear structure it is noted from the analysis that the curvilinear structure remains in compression through the depth of the foundation at the window, with the exception of the top of the window which is only slightly in tension at 1.8 psi. In addition, the maximum vertical stress in the rectangular structure is located at the left lower corner of the structure at element 1284 and measured 412.9 psi while the maximum vertical stress of the curvilinear structure, located at element 573, in the upper right corner of the window measured 38.2 psi. This represents a difference of greater than 10X in the maximum vertical stress level in the rectangular structure (Figures 8.3 and 8.4) as compared to the curvilinear structure. The maximum vertical stress for both structures was a compressive stress.

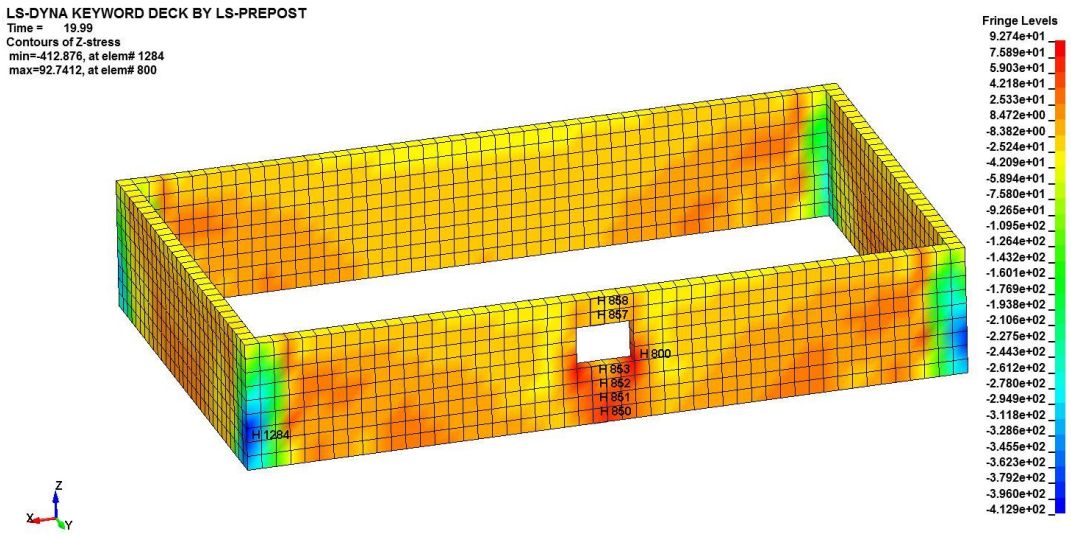

Figure 8.3: Z-Stress (Vertical) of Window Area of Rectangular Foundation – Fringe Plot

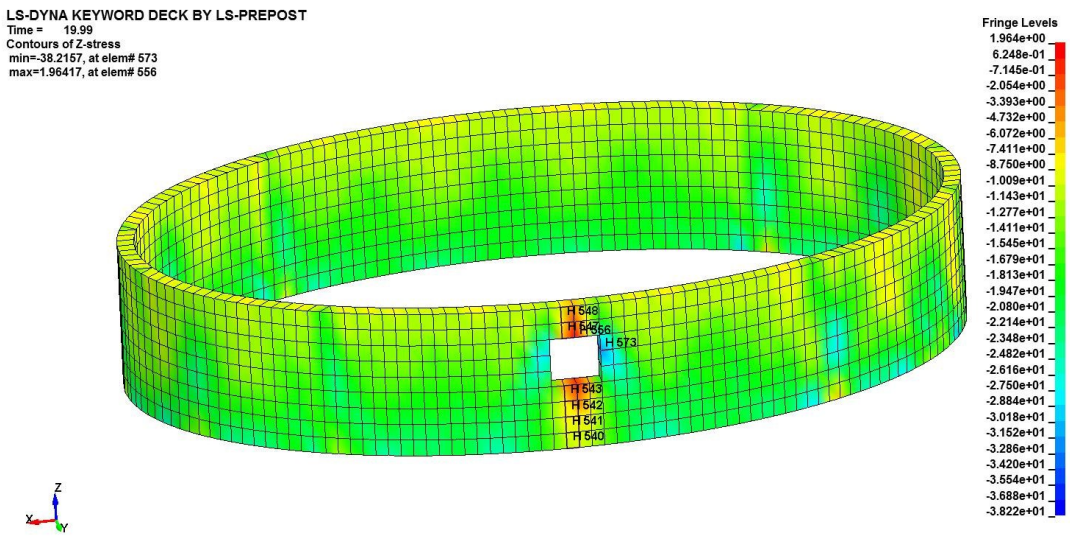

Figure 8.4: Z-Stress (Vertical) of Window Area of Curvilinear Foundation – Fringe Plot

Focusing in on the discontinuous area created by the incorporation of the window in both the rectangular structure and the curvilinear structure, the higher vertical stresses peak along the side of the window for the rectangular structure and at the upper corner of the window for the curvilinear structure (Figures 8.5 and 8.6).

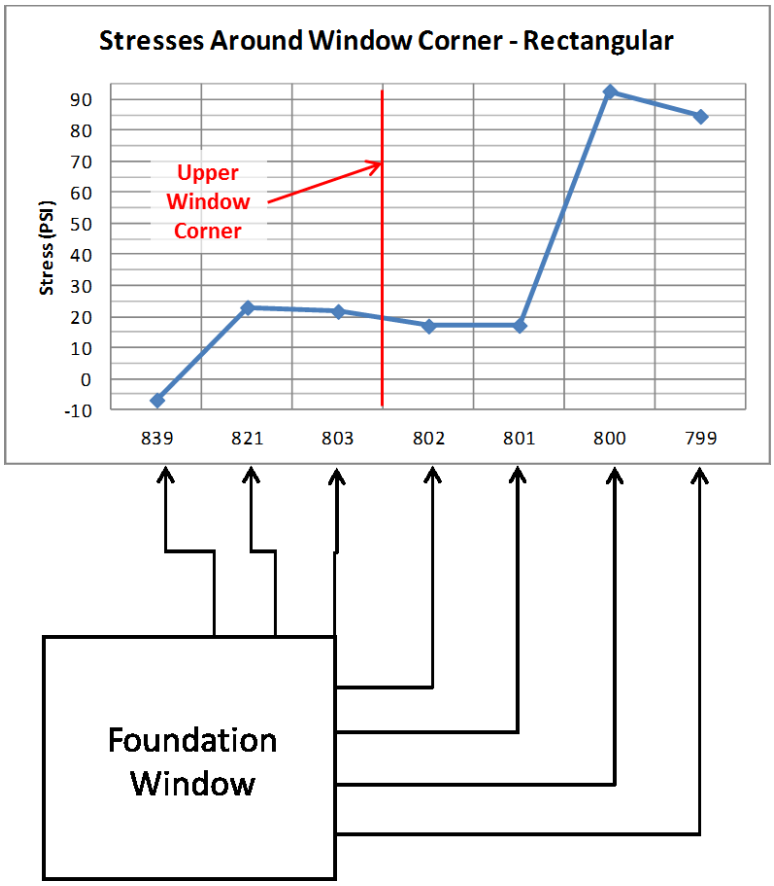

Figure 8.5: Vertical Stress around Window – Rectangular Structure

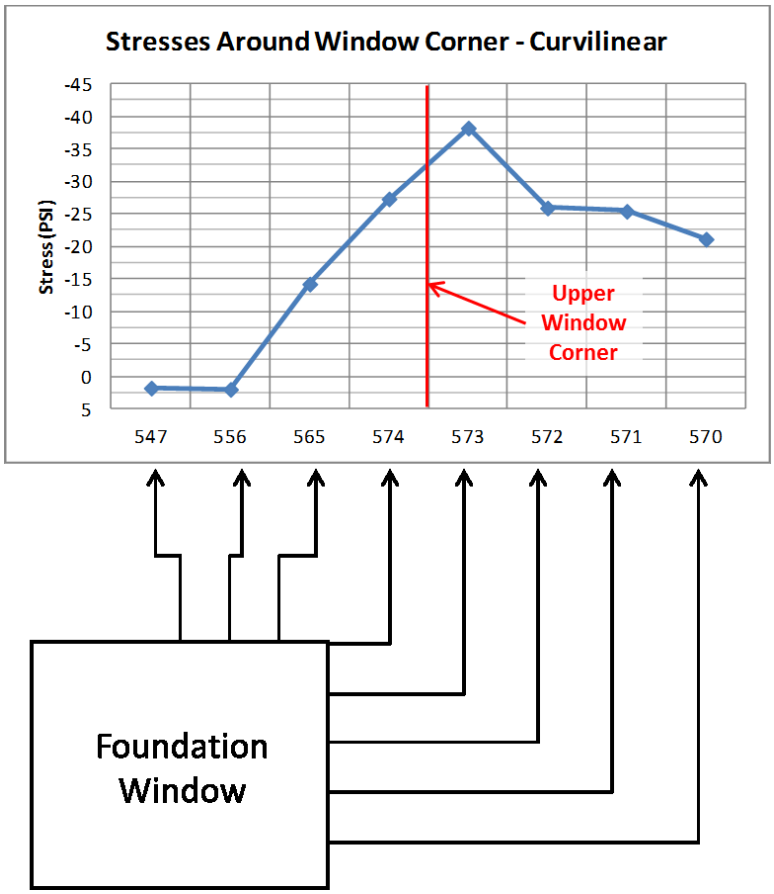

Figure 8.6: Vertical Stress around Window – Curvilinear Structure

The maximum vertical stress in the area around the window for the rectangular structure was 92.7 psi while the maximum vertical stress for the curvilinear structure for the same area was 38.2 psi. The rectangular structure around the window was primarily in tension while the curvilinear was in compression. Evaluating the stress concentration factors in that same area around the corner of the window (Table 8.3 and Table 8.4) for both the rectangular and curvilinear designs the stress concentration factors for the rectangular structure range from 0.88 to 190.18 while the curvilinear structure

ranged from 1.04 to 2.71. This represents a huge difference on structural performance relative to the applied vertical stress around the discontinuity of the window opening.

Table 8.3: Stress Concentration Factors around Window – Rectangular

Rectangular Foundation Design - Vertical Stress				
Element ID - Window	Z-Stress (psi)	Element ID - No Window	Z-Stress (psi)	Stress Concentration Factor
875	23.5	1406	-7.9	3.97
857	-7.2	1388	-7.9	0.91
839	-6.85	1370	-7.8	0.88
821	23	1352	-7.8	3.95
803	21.7	1334	-7.7	3.82
802	17	1333	-5.5	4.09
801	17.2	1332	-3	6.73
800	92.7	1331	-0.49	190.18

Table 8.4: Stress Concentration Factors around Window – Curvilinear

Curvilinear Foundation Design - Vertical Stress				
Element ID - Window	Z-Stress (psi)	Element ID - No Window	Z-Stress (psi)	Stress Concentration Factor
538	-13.4	1339	-12.9	1.04
547	1.8	1330	-13.1	1.14
556	1.9	1321	-13	1.15
565	-14.2	1312	-13.3	1.07
574	-27.3	1294	-12.6	2.17
573	-38.2	1293	-14.1	2.71
572	-25.9	1292	-14.9	1.74
571	-25.4	1291	-15.9	1.60

The performance improvement around the window in the curvilinear foundation demonstrates the advantage of designing a foundation to remain in

compression throughout the structure and the improvement in performance of crack initiation around a high stress concentration area.

8.3 Shear Stress of Foundations

When comparing the shear stress performance of the rectangular and curvilinear structures, a vertical section of wall was selected along the side of the window for each structural design. Overall, the rectangular structure exhibited much greater shear stresses for the same locations in the structure, as much as 10X for some locations (Table 8.5).

Table 8.5: Shear Stress of Rectangular and Curvilinear Wall Designs

Shear Stress Results			
Structure	Element ID	Stress (psi)	Description
Rectangular	Element 894	89.6	Top of Foundation
	Element 893	149.6	
	Element 892	52.1	
	Element 891	34.5	
	Element 890	91.8	
	Element 889	145.4	
	Element 888	62.2	
	Element 887	32.7	
	Element 886	5.4	Bottom of Foundation
Maximum shear stress in structure		235.4	
Curvilinear	Element 530	6.8	Top of Foundation
	Element 529	13.5	
	Element 528	20	
	Element 527	13.3	
	Element 526	12.4	
	Element 525	9.4	
	Element 524	12.4	
	Element 523	16.1	
	Element 522	7.6	Bottom of Foundation
Maximum shear stress in structure		21.2	

The maximum shear stress for the rectangular structure was 235.4 psi located at element 219 in the upper corner of the structure while the maximum shear stress for the curvilinear structure was 21.2 psi and was located at element 864 on the bottom of the structure (Figures 8.7 and 8.8).

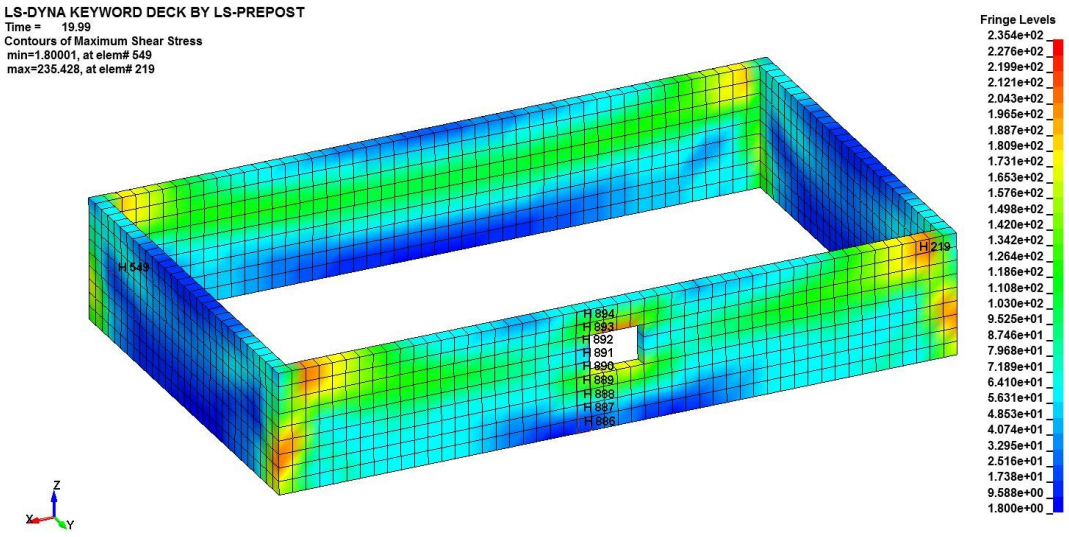

Figure 8.7: Shear Stress along Window Area of Rectangular Foundation – Fringe Plot

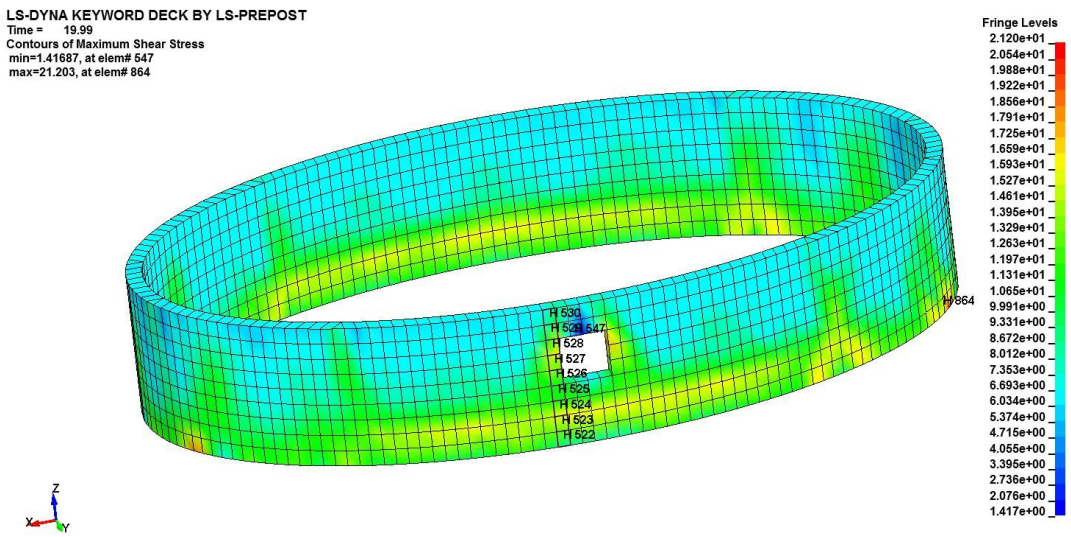

Figure 8.8: Shear Stress along Window Area of Curvilinear Foundation – Fringe Plot

Evaluating the shear stresses for the two structures around the area of discontinuity at the window, the shear stresses are greatest above the window for the rectangular structure and at the upper corner of the window for the curvilinear structure (Figures 8.9 and 8.10).

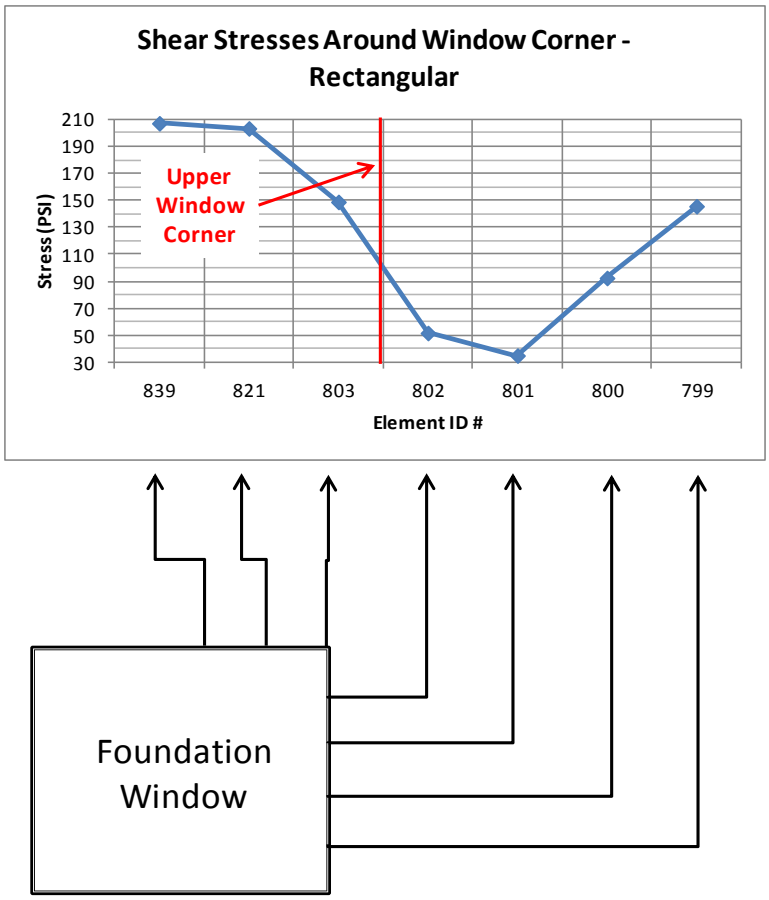

Figure 8.9: Shear Stress around Window – Rectangular Structure

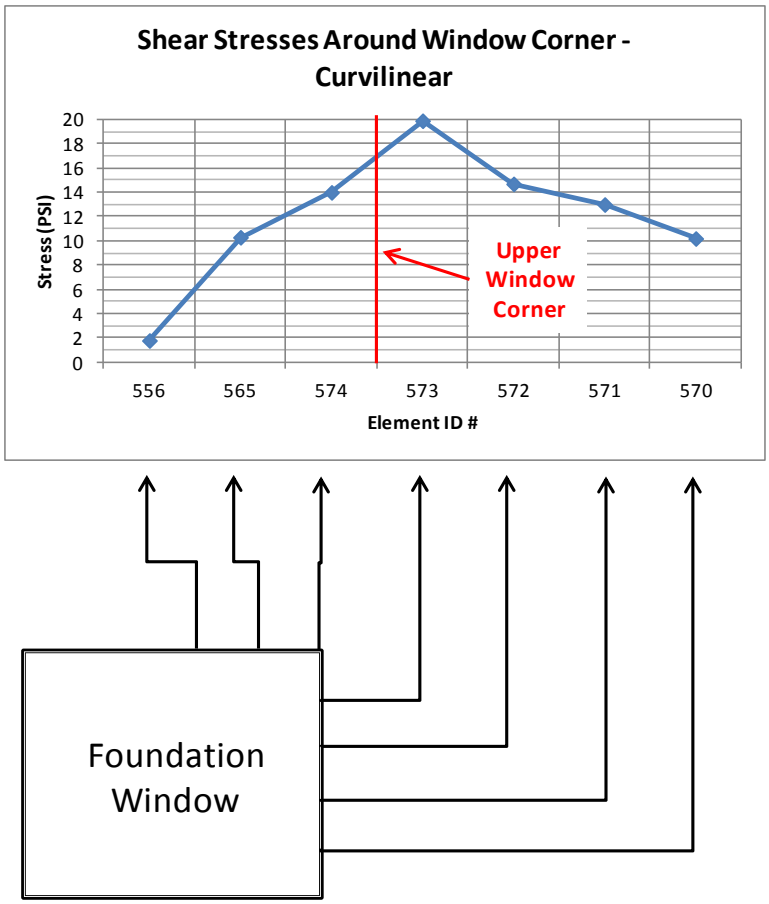

Figure 8.10: Shear Stress around Window – Curvilinear Structure

Evaluating the stress concentration factors in the same area around the corner of the window (Table 8.6 and Table 8.7), for both the rectangular and curvilinear designs, the stress concentration factors for the rectangular structure range from 61.2 to 177.8 while the curvilinear structure ranged from 6.3 to 7.8. This represents a huge difference on structural performance around the discontinuity of the window opening. Since this area of the structure is most vulnerable, due to the discontinuity of the window, the large reductions in the stress concentration factors demonstrated in the curvilinear design help to mitigate against cracking in this area.

Table 8.6: Stress Concentration Factors around Window – Rectangular

Rectangular Foundation Design - Shear Stress				
Element ID - Window	Z-Stress (psi)	Element ID - No Window	Z-Stress (psi)	Stress Concentration Factor
875	204.1	1406	61.6	3.31
857	207.6	1388	61.3	3.39
839	207.2	1370	61.2	3.39
821	203.4	1352	61.6	3.30
803	148.9	1334	62.3	2.39
802	51.7	1333	98.6	0.52
801	35	1332	177.8	0.20
800	92.5	1331	103	0.90

Table 8.7: Stress Concentration Factors around Window – Curvilinear

Curvilinear Foundation Design - Shear Stress				
Element ID - Window	Z-Stress (psi)	Element ID - No Window	Z-Stress (psi)	Stress Concentration Factor
538	10	1339	6.8	1.47
547	1.4	1330	6.6	0.21
556	1.8	1321	6.6	0.27
565	10.3	1312	6.9	1.49
574	14	1294	6.3	2.22
573	19.9	1293	7.1	2.80
572	14.7	1292	7.4	1.99
571	13	1291	7.8	1.67

9. Conclusions and Recommendations for Further Research

In the present study the analysis of a rectangular and curvilinear foundation was undertaken to demonstrate results from the evaluation of these structures under combined lateral and vertical loading confirm From the LS DYNA analysis of the rectangular and curvilinear structures, it is demonstrated that a basement foundation wall can be constructed in such a manner that all of the internal forces within the foundation are compressive forces. This design, using a curvilinear structure, takes advantage of the concrete's inherent compressive strength to resist potentially high lateral forces exerted by the soil mass. The advantage to this type of design is decreased lateral wall deflections around the circumference of the foundation leading to a better performance of the foundation even in the presence of swelling soils. The results of this study have led to several significant observations about the performance of rectangular and curvilinear structures under combined vertical and lateral loading. Key observations from the LS DYNA models are the following:

- The performance of a curvilinear structural design in light building foundations under combined lateral and vertical loading is superior to the traditional rectangular wall design. The curvilinear design remains almost entirely in compression due to the combined loading which takes advantage of the best design properties of the material.
- The curvilinear foundation design outperforms the rectangular structure by 100X when analyzed for lateral displacements under identical loading. The maximum displacement for the rectangular foundation occurred at the

right, upper corner of the window at node 1637 and measured 2.67 inches while the maximum displacement for the curvilinear structure occurred at node 1137 and measured 0.06 inches at a location above the window.

- The rectangular structure experiences both tensile and compressive forces within the structure due to the combined vertical and lateral loading. The curvilinear remains in compression throughout the structure, with the exception of the top of the window which is only slightly in tension at 1.8 psi.
- The maximum vertical stress in the rectangular structure measured 412.9 psi while the maximum vertical stress of the curvilinear structure measured 38.2 psi. This represents a difference of greater than 10X in the maximum vertical stress level in the rectangular as compared to the curvilinear structure. The maximum vertical stresses in both structures were compressive stresses.
- Evaluation of the discontinuous area created by the incorporation of the window in both structures, the higher vertical stresses peak along the side of the window for the rectangular structure and at the upper corner of the window for the curvilinear structure. The maximum vertical stress in this area around the window for the rectangular structure was 92.7 psi while the maximum vertical stress for the curvilinear structure for the same area was 38.2 psi. The rectangular structure around the window was primarily in tension while the curvilinear was in compression.

- The rectangular structure exhibited much greater shear stresses for the same locations in the structure, as much as 10X for some locations. The maximum shear stress for the rectangular structure was 235.4 psi while the maximum shear stress for the curvilinear structure was 21.2 psi.

Current mitigation techniques for expansive soils include adjusting drainage, underpinning or mitigation of the design by using pier and beam foundations with drainage implemented at the foundation to prevent soil expansion. These strategies assume a stable soil condition over the life of the foundation and do not take into account the potential changing soil conditions at the foundation wall over time. Incorporating a design that resists the forces exerted by a swelling soil ensures survivability of the structure even if drainage fails and expansive soils are present at the foundation.

Although the current industry standards for mitigation of light structures constructed in expansive soils, as described above, offer piece of mind against catastrophic damage, long term stability is not guaranteed. Over time, severe drought and flooding cycles can directly influence the foundation performance and exceed the design mitigations implemented. In addition, changes in soil chemistry can occur during periods of high moisture exposure negating the benefits of soil treatment methodologies. Over time, changes in soil drying can occur due to rises in the ambient temperatures and/or the growth of vegetation within the soil mass. With unprecedented weather events taking place all over the globe, the design of structures must rely less on mitigation of moisture

intrusion and more on foundation designs that take advantage of the potential forces mobilized by the soil.

Based on the present work additional analysis is required in the finite element analysis of the two structural types. The following are recommendations for continued research:

- A better understanding of the sensitivity of the ellipse dimensions versus the introduction of tensile forces within the structural wall would be helpful in refining the design for the optimum use of space and constructability.
- The development of an expansive soil model in LS DYNA to provide a more accurate soil model that takes into consideration the saturation state of the soil and the changing soil pressures as a function of moisture content and density would help in more accurate modeling of the lateral forces. This should be combined with experiments that validate the soil model and the LS DYNA results.
- A more accurate modeling the reinforced concrete foundation by incorporating the rebar reinforcement using beam elements within the solid element structure of the concrete. This would replace the smeared properties used in this analysis.
- The introduction of piers for the foundation support would complete the design model for the curvilinear foundation and enable the analysis of a complete foundation system.

- The experimental derivation of the static and dynamic coefficients of friction between the subject soil and concrete foundation to more accurately model the physical contact.

REFERENCES

American Concrete Institute. (2005). *Building Code Requirements for Structural Concrete (ACI 318-05)*. Farmington Hills, MI.

American Society of Civil Engineers. (2005). Minimum Design Loads for Buildings and Other Structures. Danvers, MA.

Das, B. M. (2002). Soil mechanics laboratory manual. (6th ed.). New York: Oxford University Press.

Donaldson, G. W. (1969). The Occurrence of Problems of Heave and the Factors Affecting its Nature. 2nd International Research and Engineering Conference on Expansive Clay Soils. Texas Press.

ETL 1110-3-446, 1992, Department of the Army, U.S. Army Corps of Engineers, Engineering and Design Revision of Thrust Block Criteria in TM 5-813-5/AFM 88-10, Vol. 5, Appendix C, Department of the Army, Washington, D.C.

Grim, R. E. (1968). Clay Mineralogy: International Series in the Earth and Planetary Sciences. New York: McGraw-Hill Book Company.

Hardy, R. M. (1965). Identification and Performance of Swelling Soil Types. *Canadian Geotechnical Journal, 11*, (2),141-161.

Holtz, W.G., and Gibbs, H.J. (1956). Engineering properties of expansive clays. *Transactions of ASCE, 121*, 641-663.

Holtz, R. D., and Kovacs, W. D. (1981). *An Introduction to Geotechnical Engineering.* New Jersey: Prentice Hall.

International Code Council. (2006). *International Building Code.* Country Club Hills, IL.

International Code Council. (2006). *International Residential Code for One and Two-Family Dwellings.* Country Club Hills, IL.

Howard, A. K. (1977). Laboratory Classification of Soils: Unified Soil Classification System. *Earth Sciences Training Manual, no. 4, U.S. Bureau of Reclamation, Denver, CO.*

Jones, D.E J., and Holtz, W.G. (1973) Expansive Soils – The hidden Disaster. *Civil Engineering*, 43.

Lambe, T. W. (1953) The Structure of Inorganic Soil. *Proceedings of the American Society of Civil Engineers*, 79, (pp. 49).

Lambe, T. W. and Whitman, R. V. (1969), *Soil Mechanics*. New York: John Wiley & Sons.

McCarthy, David F. (1998). *Essentials of Soil Mechanics and Foundations*. Columbus, Ohio: Prentice Hall.

Mitchel J. K. (1976). *Fundamentals of Soil Behaviour.* New York: John Wiley & Sons.

Mitchel J. K. (1993). *Fundamentals of Soil Behaviour.* (2^{nd} ed.). New York: John Wiley & Sons.

Nelson, J. D., and Miller, D. J. (1992). *Expansive Soils, Problems and Practice in Foundation and Pavement Engineering*, New York: John Wiley & Sons.

Seed, H. B., Woodward, R. J., and Lundgren, R. (1962) Prediction of Swelling Potential for Compacted Clays: *ASCE Journal of Soil Mechanics and Foundations Division*, SM-3, Part 1, 53-87.

Skempton, A.W. (1953). The Colloidal Activity of Clay. *Proceedings of the Third International, Conference on Soil Mechanics and Foundation Engineering*,*1*, 57 – 60.

Steinberg, M. (1998). *Geomembranes and the Control of Expansive Soils in Construction*. New York: McGraw-Hill.

U.S. Army Corps of Engineers. (1970). *Laboratory Soils Testing*, EM 1110-2-1906, Appendix V.